Article

Current Biology

Phasic Dopamine Signals in the Nucleus Accumbens that Cause Active Avoidance Require Endocannabinoid Mobilization in the Midbrain

Highlights

- Optogenetic stimulation of midbrain dopamine cells enhances active avoidance
- Accumbal D1 antagonism diminishes avoidance
- Midbrain endocannabinoid antagonism attenuates avoidance and dopamine release
- Well-learned avoidance is no longer controlled by this endocannabinoid/dopamine signal

Authors

Jennifer M. Wenzel, Erik B. Oleson, Willard N. Gove, ..., Sachin Patel, Carl R. Lupica, Joseph F. Cheer

Correspondence

jcheer@som.umaryland.edu

In Brief

Wenzel et al. demonstrate that phasic mesolimbic dopamine promotes behavior motivated by a cue that predicts a negative event. This dopamine signal is controlled by midbrain endocannabinoids. However, once this behavior is well learned, it becomes independent of these systems.

Wenzel et al., 2018, Current Biology *28*, 1–13
May 7, 2018
https://doi.org/10.1016/j.cub.2018.03.037

CellPress

Please cite this article in press as: Wenzel et al., Phasic Dopamine Signals in the Nucleus Accumbens that Cause Active Avoidance Require Endocannabinoid Mobilization in the Midbrain, Current Biology (2018), https://doi.org/10.1016/j.cub.2018.03.037

Current Biology
Article

Phasic Dopamine Signals in the Nucleus Accumbens that Cause Active Avoidance Require Endocannabinoid Mobilization in the Midbrain

Jennifer M. Wenzel,[1] Erik B. Oleson,[2] Willard N. Gove,[1] Anthony B. Cole,[1] Utsav Gyawali,[3] Hannah M. Dantrassy,[1] Rebecca J. Bluett,[4] Dilyan I. Dryanovski,[5] Garret D. Stuber,[6] Karl Deisseroth,[7] Brian N. Mathur,[3] Sachin Patel,[4,8] Carl R. Lupica,[5] and Joseph F. Cheer[1,9,10,11,*]

[1]Department of Anatomy and Neurobiology, University of Maryland School of Medicine, Baltimore, MD 21201, USA
[2]Department of Psychology, University of Colorado, Denver, CO 80204, USA
[3]Department of Pharmacology, School of Medicine, University of Maryland, Baltimore, MD 21201, USA
[4]Vanderbilt Brain Institute and Department of Psychiatry, Vanderbilt University, Nashville, TN 37235, USA
[5]Electrophysiology Research Section, Cellular Neurobiology Branch, National Institute on Drug Abuse, Intramural Research Program, NIH, Baltimore, MD 21224, USA
[6]Department of Psychiatry and Neuroscience Center, University of North Carolina at Chapel Hill, Chapel Hill, NC 27514, USA
[7]Department of Bioengineering, Stanford University, Stanford, CA 94305, USA
[8]Vanderbilt School of Medicine and Department of Molecular Physiology and Biophysics, Vanderbilt University Medical Center, Nashville, TN 37235, USA
[9]Department of Psychiatry, University of Maryland School of Medicine, Baltimore, MD 21201, USA
[10]Program in Neuroscience, University of Maryland School of Medicine, Baltimore, MD 21201, USA
[11]Lead Contact
*Correspondence: jcheer@som.umaryland.edu
https://doi.org/10.1016/j.cub.2018.03.037

SUMMARY

Phasic dopamine (DA) release accompanies approach toward appetitive cues. However, a role for DA in the active avoidance of negative events remains undetermined. Warning signals informing footshock avoidance are associated with accumbal DA release, whereas depression of DA is observed with unavoidable footshock. Here, we reveal a causal role of phasic DA in active avoidance learning; specifically, optogenetic activation of DA neurons facilitates avoidance, whereas optical inhibition of these cells attenuates it. Furthermore, stimulation of DA neurons during presentation of a fear-conditioned cue accelerates the extinction of a passive defensive behavior (i.e., freezing). Dopaminergic control of avoidance requires endocannabinoids (eCBs), as perturbing eCB signaling in the midbrain disrupts avoidance, which is rescued by optical stimulation of DA neurons. Interestingly, once the avoidance task is learned, neither DA nor eCB manipulations affect performance, suggesting that once acquisition occurs, expression of this behavior is subserved by other anatomical frameworks. Our findings establish an instrumental role for DA release in learning active responses to aversive stimuli and its control by eCB signaling.

INTRODUCTION

To survive, organisms must learn how to interact appropriately with their environment—i.e., to approach positive stimuli, to avoid triggers that predict negative events, and to engage in passive defensive behaviors when danger is unavoidable. Such adaptive behaviors are continually guided by the mesolimbic dopamine (DA) system, originating in the ventral tegmental area (VTA) and projecting to regions such as the prefrontal cortex (PFC) and nucleus accumbens (NAc) [1, 2]. Burst firing of DA neurons and phasic accumbal DA release accompany appetitive stimuli [3–5]. Conversely, aversive stimuli suppress DA cell firing and accumbal DA release [4, 6–8]. After repeated presentation, coincident DA activity shifts from stimulus presentation to the earliest predictive cue—leading to the notion that DA release is a substrate for cue-directed appetitive behavior [9]. Indeed, optogenetic activation of DA neurons at either appetitive cue presentation or reward delivery modulates cue-stimulus learning [10] and enhances cue-induced responding [11].

The role of phasic DA in aversively motivated behaviors, however, is much less clear. Our prior fast-scan cyclic voltammetry (FSCV) studies revealed patterned phasic DA release in NAc core (NAcC) during footshock avoidance [8]. In this task, a warning signal (WS) precedes footshock. Rats can lever press to either avoid footshock onset or to escape ongoing footshock. We found that phasic DA release in NAcC at the WS reliably predicted successful avoidance [8]. This release pattern is analogous to that seen with appetitive cues and is thus hypothesized to reflect an animal's expectation that shock is avoidable (safety is attainable) [12, 13], driving active avoidance. Conversely, DA release was decreased at the WS prior to escape [8]. This pause most likely signals an impending unavoidable aversive stimulus. Indeed, the presentation of a cue previously paired with unavoidable footshock produced similar decreases in DA release, which coincided with freezing behavior [6, 8]. Moreover, extinction of freezing was accompanied by re-established baseline DA release patterns. These data suggest that augmented cue-evoked DA release in the NAcC may cause active avoidance

of aversive stimuli, i.e., negative reinforcement. Conversely, reduced DA release may promote passive defensive behaviors (e.g., freezing) when unavoidable aversive stimuli are present.

Here, we utilize optogenetics to examine a causal role for DA release in the response to aversive cues. Voltammetric measurements allowed us to identify a physiologically relevant stimulation capable of mimicking DA release observed prior to avoidance. We find that optical emulation of these DA release patterns enhanced avoidance, whereas optogenetic inhibition of DA cells diminished it. Notably, stimulation of midbrain DA cells enhanced extinction of cue-evoked conditioned fear, revealing a role for dopamine in the promotion of active over passive defensive behaviors (e.g., freezing).

Given the fundamental role of endocannabinoids (eCBs) in shaping phasic activity of VTA DA neurons in response to positive stimuli/cues [8, 14], we further hypothesized that eCBs mediate avoidance behavior and associated DA release. Indeed, disruption of VTA eCB signaling attenuated DA release to the WS and active avoidance whereas optogenetic activation of DA neurons rescued avoidance responding following CB1 receptor blockade, restricting the observed pharmacological effects to DA neurons. Interestingly, once the avoidance task is well learned, animals are no longer susceptible to DA or eCB manipulations on avoidance behavior, suggesting a time-dependent role for these systems in learning to avoid aversive stimuli.

RESULTS

Optogenetic Stimulation of DA Neurons Enhances Active Avoidance

To examine a causal role of phasic DA in avoidance behavior, we expressed either the excitatory opsin channelrhodopsin-2 (ChR2) (TH::Cre+ n = 5; TH::Cre− n = 5) or the inhibitory opsin, Halorhodopsin (NpHR) (TH::Cre+ n = 5; TH::Cre− n = 5), in the VTA and implanted bilateral optical fibers.

Rats learned an operant shock avoidance procedure as in our previous work [8]. Briefly, a WS cue was presented 2 s before the onset of footshock. A single lever press during this initial 2 s resulted in footshock "avoidance," whereas a lever press made after shock initiation resulted in "escape." Either response initiated a 20 s no-shock "safety" period. Animals were trained until they reached stable avoidance with a mean percent avoidance ([no. of avoidance responses / total number of responses] × 100) of approximately 50% (Figure 1A).

At ~50% avoidance, rats underwent a single test session consisting of a 30 min no-stimulation baseline and 30 min in with laser stimulation at the WS (segments were counterbalanced). For ChR2, laser stimulation (ten pulses, 20 Hz) closely approximated phasic DA release measured during avoidance [8, 15] (Figure S1; Video S1). To inhibit VTA DA cells, we applied 3 s of laser light beginning 2 s prior to the WS [16, 17]. For ChR2, ANOVA revealed an effect of stimulation ($F_{1,8}$ = 22.501, p = 0.001) and interaction ($F_{1,8}$ = 24.282, p = 0.001). Aligned with our previous work, post hoc comparisons showed that stimulation significantly enhanced avoidance in TH::Cre+ rats (p = 0.006), but not controls (p > 0.05; Figure 1B). For NpHR, ANOVA revealed an effect of stimulation ($F_{1,7}$ = 29.5, p = 0.001), genotype ($F_{1,7}$ = 13.492, p = 0.008), and an interaction ($F_{1,7}$ = 45.100, p < 0.001). Post hoc tests confirmed that inhibition of DA cells diminished avoidance in TH::Cre+ animals (p = 0.001), but not controls (p > 0.05; Figure 1C).

NAcC D1, but Not D2, Receptor Antagonism Attenuates Active Avoidance

Given our prior FSCV results [8], we hypothesized that DA release specifically within the NAcC facilitates avoidance. To test this, another group of rats (n = 5) were transduced with ChR2 in the VTA and received bilateral optical fibers in the NAcC. After training to 50% avoidance, rats performed a single avoidance test session, composed of a 15 min baseline and 15 min with laser stimulation at the WS. Stimulation of NAcC DA terminals significantly enhanced avoidance (t_4 = −4.06, p = 0.015; Figure 1D).

Another major terminal field of the mesolimbic system is the PFC [18], and DAergic activity in PFC is believed to control goal-directed responding [19]. However, unlike in the NAcC, PFC neurons are not thought to directly encode DAergic cue-response signals [20]. Moreover, lesioning prelimbic PFC does not affect the acquisition of active avoidance [21]. Therefore, we hypothesized that, unlike the NAcC, phasic DA signaling within the PFC does not facilitate avoidance. To test this, rats were transduced with ChR2 in the VTA and received bilateral optical fibers in the PFC (n = 5), after which they underwent an identical training and testing protocol. Unlike that observed with NAcC DA terminal stimulation, PFC terminal stimulation did not enhance avoidance (p > 0.05; Figure 1E). We confirmed the ability of terminal stimulation to release DA in the NAcC and PFC using *ex vivo* FSCV in brain slices (Figure 1F) [10].

D1 receptors have low affinity and thus are believed to be primarily responsible for transducing phasic high-concentration DA fluctuations [22]; therefore, we hypothesized that NAcC D1 signaling mediates laser facilitation of avoidance. TH::Cre+ rats (n = 7) received ChR2, bilateral optical fibers in the VTA, and bilateral guide cannulae aimed at the NAcC. Rats were trained to ~50% avoidance and then underwent two test sessions consisting of a 10 min baseline followed by intra-NAcC infusion of vehicle (VEH) or the D1 receptor antagonist SCH23390 (SCH; 0.25 μg/side). Animals then performed 10 min of the task without laser stimulation followed by 10 min with laser stimulation at the WS. ANOVA showed a main effect of treatment ($F_{5,30}$ = 3.01, p = 0.029; Figure 1G), and post hoc tests revealed that while intra-NAcC VEH did not alter avoidance, stimulation enhanced avoidance (p = 0.002). Importantly, this dose of intra-NAcC SCH did not attenuate avoidance (p > 0.05) but prevented laser-induced increases. To corroborate our terminal stimulation findings, SCH infusion into the PFC did not affect baseline avoidance nor did SCH attenuate laser facilitation of avoidance (Figure 1H). ANOVA revealed a significant effect of stimulation ($F_{5,25}$ = 3.76, p = 0.011), and post hoc comparisons showed that laser in conjunction with either VEH (p = 0.012) or SCH (p = 0.003) enhanced avoidance.

Previous reports show that disrupting NAcC DA signaling suppresses avoidance [23, 24]. Therefore, we tested two higher doses of SCH to fully examine NAcC D1 signaling in our avoidance task. Rats (n = 9) received bilateral guide cannulae aimed at the NAcC and were trained to ~50% avoidance, after which they underwent two test sessions, composed of a 15 min baseline and then intra-NAcC infusion of VEH (n = 9) on one day and a

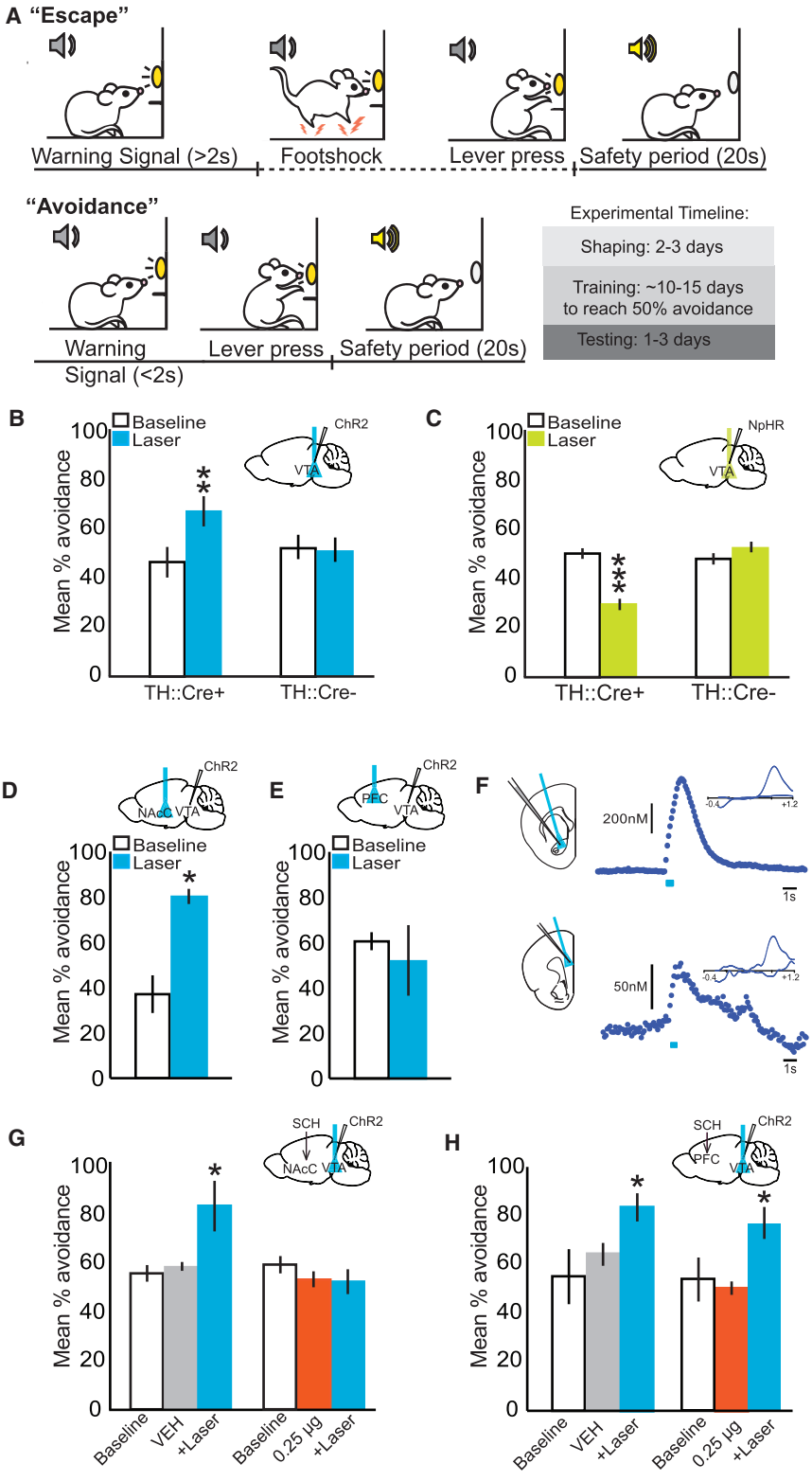

Figure 1. Optogenetic Stimulation of DA Neurons Enhances Active Avoidance

(A) Experiment timeline.

(B) Mean percent avoidance during baseline and laser stimulation of VTA DA cells.

(C) Avoidance during baseline and laser inhibition of VTA DA cells.

(D) Avoidance during baseline and laser stimulation of NAcC DA terminals.

(E) Avoidance during baseline and laser stimulation of PFC DA terminals.

(F) Representative FSCV dopamine trace and corresponding cyclic voltammogram illustrating the ability of NAcC and PFC terminal stimulation to release DA.

(G) Avoidance in rats receiving stimulation of the VTA following intra-NAcC VEH or SCH.

(H) Avoidance in rats receiving stimulation of the VTA following intra-PFC VEH or SCH.

Insets in (B)–(H) show rat brain indicating viral transduction in VTA, placement of optical fibers (blue/yellow), and/or location of infusion. Error bars are ±SEM;*$p \leq 0.05$, ***$p \leq 0.001$. See also Figure S1 and Video S1.

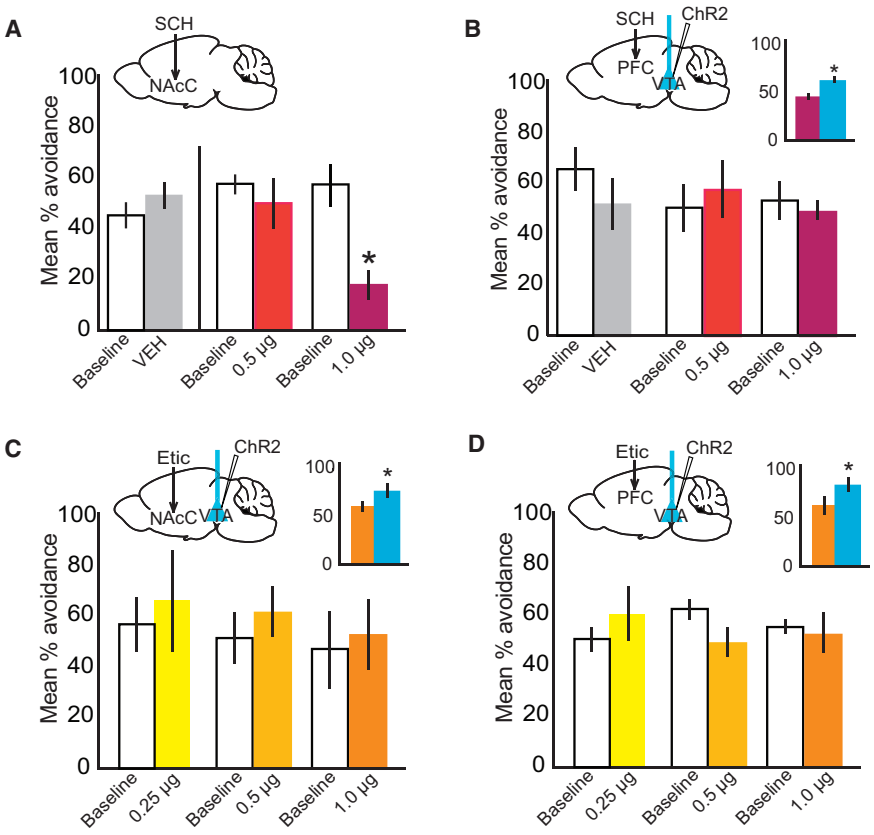

Figure 2. NAcC D1, but Not D2, Receptor Antagonism Attenuates Active Avoidance

(A) Mean percent avoidance during baseline and following intra-NAcC infusion of one of two doses of SCH or VEH.

(B) Avoidance during baseline and following bilateral intra-PFC infusion of SCH or VEH. Inset shows that, following SCH (1.0 μg/side), VTA stimulation significantly increased avoidance (blue bar).

(C) Avoidance during baseline and following intra-NAcC infusion of one of three doses of eticlopride (Etic). Inset shows that following Etic (1.0 μg/side), VTA stimulation increased avoidance (blue bar).

(D) Avoidance during baseline and following intra-PFC infusion of three doses of Etic. Inset shows that, following 1.0 μg/side Etic, VTA optical stimulation significantly increased avoidance (blue bar). Insets show illustrations of rat brain indicating VTA ChR2 transduction, placement of optical fibers (blue), and/or location of SCH or Etic infusion. Error bars are ±SEM; *$p \leq 0.05$.

dose of SCH (0.5 μg/side [n = 5] or 1.0 μg/side [n = 4]) on another day (Figure 2A). VEH did not alter avoidance responding ($p > 0.05$). ANOVA showed significant main effects of SCH dose ($F_{1,7} = 7.654$, $p = 0.28$) and treatment ($F_{1,7} = 9.532$, $p = 0.018$), and post hoc comparisons showed that the highest dose of SCH significantly attenuated avoidance (one-tailed t test, $t_3 = 2.541$, $p = 0.0425$) as predicted by our prior findings that the WS engenders a large DA transient that accompanies successful avoidance [8], as well as the work of others indicating a general role for accumbal DA in avoidance [23, 24]. However, intra-PFC SCH (n = 4) had no effect on baseline responding at any dose tested ($p > 0.05$) and did not block laser-induced increases in avoidance even at the highest dose ($t_3 = 3.323$, $p = 0.045$; Figure 2B). Similarly, infusion of the D2 receptor antagonist eticlopride into the NAcC (n = 4; Figure 2C) or the PFC (n = 4; Figure 2D) had no effect on baseline avoidance at any of the three doses tested (0.25, 0.5, or 1.0 μg/0.5 μL/side; $p > 0.05$). Furthermore, laser stimulation of VTA DA cell bodies at the WS continued to facilitate avoidance following infusion of the highest dose of eticlopride into either the NAcC ($t_2 = -4.564$, $p = 0.045$) or the PFC ($t_3 = -3.508$, $p = 0.039$).

Laser Stimulation of DA Cells Promotes Cue-Induced Approach

We theorize that DA release increases active avoidance directed by the WS. However, it may be that DAergic stimulation engages an "approach" motor program, independent of cues. To test this, we trained animals under a variable time out (VTO) schedule for food. VTO schedules typically result in animals disengaging from the lever [25, 26], enabling us to test how stimulation and cue presentation separately affect approach. For this, TH::Cre+ rats with ChR2 and bilateral optical fibers in the VTA (n = 8) learned an FR1 schedule for food in which reward availability (signaled by a cue light) was variable. Upon stable responding, animals underwent two 30 min test sessions, interleaved with baseline sessions. On test session 1, laser stimulation was delivered coincident with cue presentation (to test the ability of stimulation to facilitate cue-induced approach). On test session 2, laser stimulation was delivered midway through the VTO (to test the ability of stimulation to facilitate approach independent of cues; Figure 3A). Animals did not differ in the number of pellets earned for any session ($p > 0.05$; data not shown), and all pellets were consumed. As expected, stimulation reduced response latency when presented in conjunction with an appetitive cue ($F_{3,21} = 16.97$, $p = 0.022$; Figure 3B) [15], and stimulation not coincident with cue presentation did not expedite cue-induced responding ($p > 0.05$; Figure 3B). Video analysis confirmed that stimulation itself does not cause either orienting toward the lever or a press (n = 6). Indeed, when stimulation was dissociated from the cue (i.e., when it was presented during the VTO), animals had a longer latency to either orient to ($t_5 = -6.91$, $p = 0.001$) or press the lever ($t_5 = -13.76$, $p < 0.001$), compared to when laser was coincident with the cue (Figures 3C and 3D). Therefore, optogenetic stimulation of DA neurons does not initiate an approach sequence independent of cues.

Optogenetic Stimulation of DA Neurons Facilitates the Extinction of Conditioned Fear

It remains unknown how pauses in DA activity influence defensive behavior. Nevertheless, decreases in phasic NAcC DA release correlate with freezing [6, 8]. We hypothesized that optogenetic activation of DA neurons at the presentation of an aversively conditioned cue would reverse cue-induced decreases in DA to diminish conditioned freezing. TH::Cre+ (n = 7) and

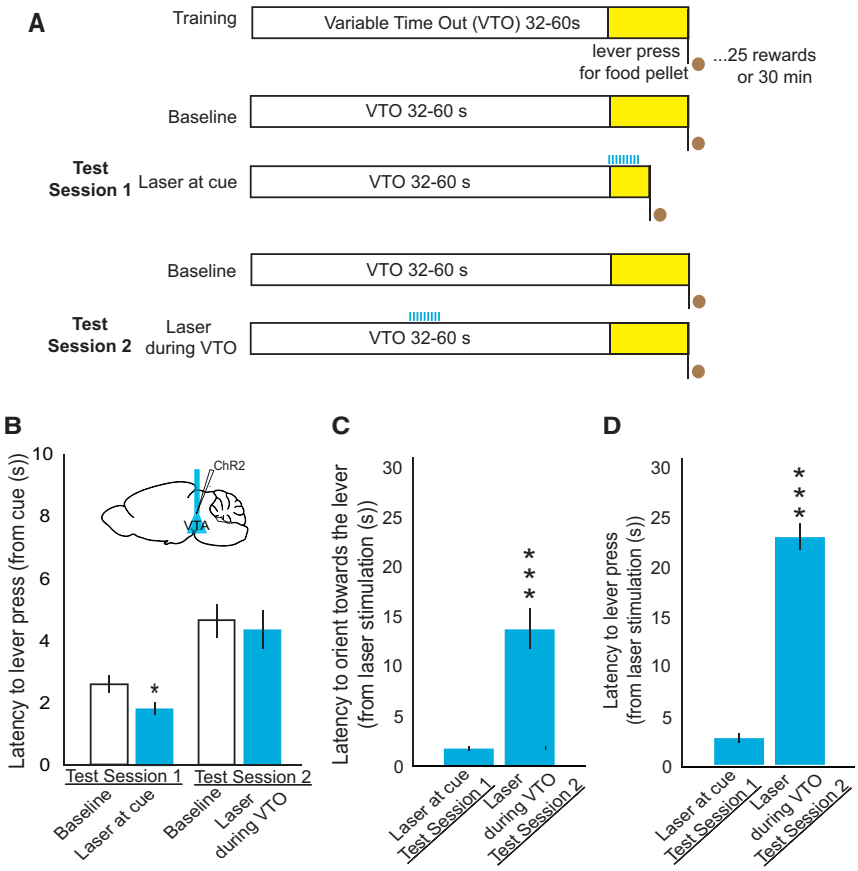

Figure 3. Laser Stimulation of DA Cells Specifically Promotes Cue-Induced Approach

(A) Schematic of VTO procedure.

(B) Latency from cue light presentation to lever press for food. Inset shows infusion of ChR2 and implantation of bilateral optical fibers in the VTA.

(C) Latency from laser stimulation to orient to either the lever, food receptacle, or cue light.

(D) Latency from stimulation to lever press.

Error bars are ±SEM; *p ≤ 0.05, ***p ≤ 0.001.

TH::Cre− control (n = 6) rats received ChR2 and bilateral optical fibers in the VTA (Figure 4A). An additional control group of TH::Cre− rats (n = 6) received no viral transduction or laser stimulation to control for nonspecific effects of virus or laser. Because statistical analysis revealed no difference between these control groups, here they are combined into a single "TH::Cre−" group (n = 11). Animals experienced a three-day fear conditioning/extinction procedure. On day 1, rats were conditioned to associate a tone with footshock. On day 2, rats underwent extinction to the conditioned cue in a novel environment, during which cue presentation coincided with optical stimulation (ten pulses, 20 Hz, 2 s intervals). Day 3 was identical to day 2 except animals did not receive stimulation (Figure 4B). Our published data [8] show that animals exhibit the most freezing and cue-associated depression of DA transients during the first third of the extinction session, so we averaged counts of freezing across session thirds. Both groups began day 2 with similar levels of freezing ($p > 0.05$). ANOVA revealed a main effect of trial ($F_{2,32} = 6.224$, $p = 0.005$), indicating that freezing decreased as the session continued (Figure 4C). There was also a significant main effect of genotype ($F_{1,16} = 5.398$, $p = 0.034$), confirming that stimulation of VTA DA neurons in TH::Cre+ rats accelerated the extinction of conditioned freezing on day 2.

Crucially, on day 3 (Figure 4D), TH::Cre+ rats continued to exhibit significantly less conditioned freezing in the absence of stimulation. ANOVA revealed main effects of trial ($F_{2,32} = 17.443$, $p < 0.001$) and genotype ($F_{1,16} = 4.798$, $p = 0.044$) with an interaction ($F_{2,32} = 4.084$, $p = 0.026$). Although TH::Cre+ animals do not freeze less on the first trial, they show a rapid decline in freezing over the first six trials to reach a significantly reduced level of freezing compared to controls ($p = 0.01$). Thus, stimulation of VTA DA neurons enduringly reduces freezing to an aversively conditioned cue, thereby enhancing extinction of conditioned fear. Importantly, these data cannot be explained by locomotor-enhancing effects of laser stimulation ($p > 0.05$; Figure 4F).

Antagonism of eCB Signaling Attenuates Active Avoidance and the DA Response to the WS

The eCB system is critically involved in the regulation of phasic DA, and its disruption curtails DA-dependent appetitive behavior [27]. We thus hypothesized that CB1 receptor antagonism would decrease avoidance. Rats (n = 5) were implanted with jugular catheters and trained to ~50% avoidance. Before each of three 30 min test sessions, rats received either intravenous (i.v.) VEH (a 1:1:18 mixture of ethanol:alkamuls:saline) or rimonabant (0.56 mg/kg or 1.0 mg/kg). In support of our hypothesis, ANOVA revealed a significant effect of rimonabant ($F_{2,8} = 14.080$, $p = 0.002$; Figure 5A), and post hoc tests confirmed a significant reduction in avoidance following either dose ($p = 0.011$, $p = 0.012$).

To determine whether rimonabant similarly disrupted DA release at the WS, another group of rats (n = 5) received jugular catheters and voltammetric electrodes aimed at the NAcC. We recorded NAcC DA release following i.v. VEH and cumulative dosing of rimonabant (Figure 5B). ANOVA revealed that rimonabant markedly reduced DA release coincident with the WS ($F_{2,8} = 8.872$, $p = 0.009$), and post hoc tests revealed both doses significantly decreased DA compared to VEH ($p = 0.035$, $p = 0.036$). These data suggest that disruption of CB1 signaling attenuates avoidance through disruption of cue-induced NAcC DA release. This finding aligns with work by Marsicano and colleagues [28], showing that rimonabant prevents the extinction of conditioned freezing, an effect that would prohibit the expression of active avoidance.

eCBs are theorized to potently modulate the dynamic range of DA neuron activity through actions in the VTA [29–31]. We sought to directly examine the role of VTA eCB function in avoidance.

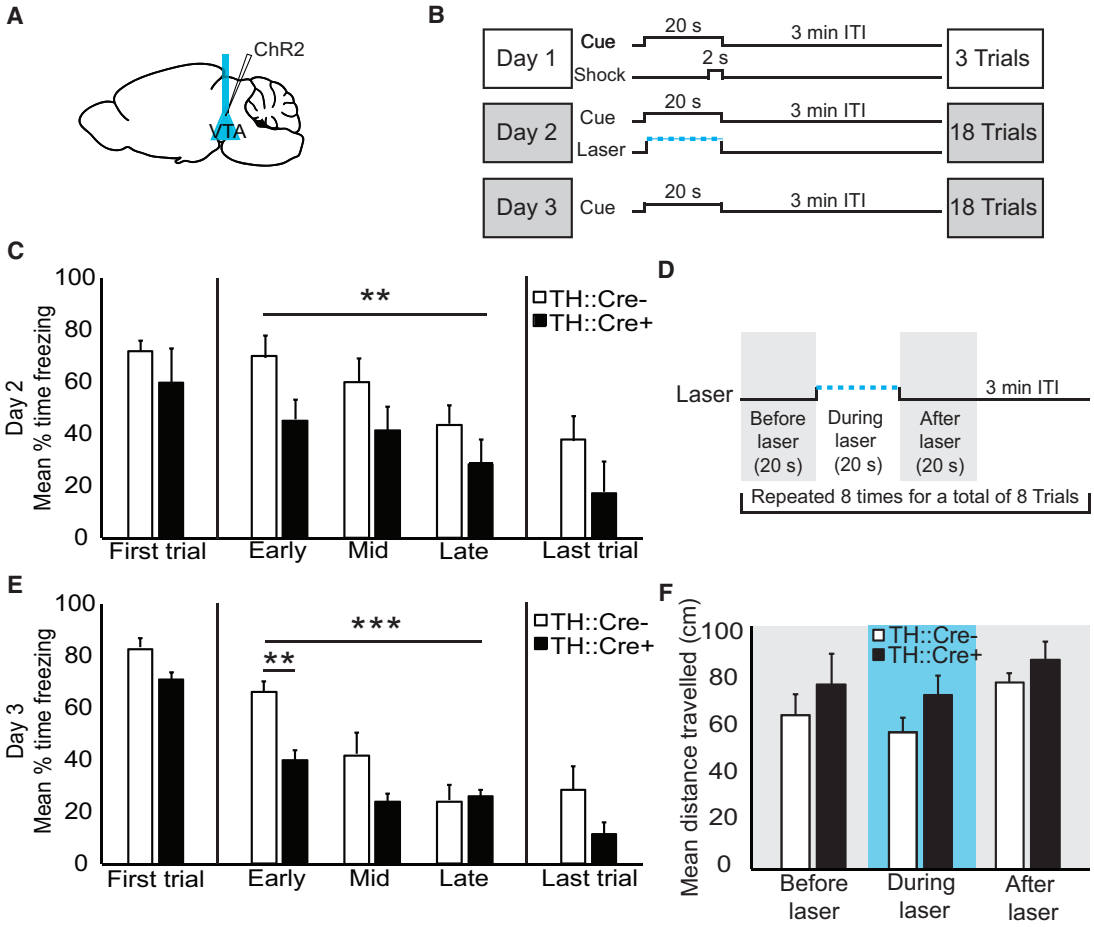

Figure 4. Optogenetic Stimulation of DA Neurons Facilitates the Extinction of Conditioned Fear

(A) Illustration of rat brain indicating placement of VTA optical fibers and ChR2 transduction.

(B) Depiction of fear conditioning and extinction protocol. Days 2 and 3 are shaded to denote a unique environment.

(C) Mean time spent freezing during the presentation of the conditioned cue on day 2. Trials (cue presentations) have been averaged into thirds of the session: "early" (trials 1–6); "mid" (trials 7–12), and "late" (trials 13–18).

(D) Mean time spent freezing during presentation of the conditioned cue on day 3.

(E) Illustration of locomotor activity test.

(F) Mean distance traveled.

Error bars are +SEM; $^{**}p \leq 0.01$, $^{***}p \leq 0.001$.

Rats (n = 5) received bilateral guide cannulae aimed at the VTA, were trained to ~50% avoidance, and underwent three test sessions. For the first 15 min, animals performed the task at baseline. Each test sessions' baseline did not differ ($p > 0.05$), so they were averaged together (Figure 5C). Rats then received an intra-VTA infusion of either VEH (1:1:18, ethanol:alkamuls: aCSF) or rimonabant (0.20 μg/side or 1.0 μg/side). As expected, intra-VTA rimonabant administration attenuated avoidance. ANOVA revealed a significant main effect ($F_{3,12} = 14.51$, $p < 0.001$), and post hoc comparisons showed that 1.0 μg/side rimonabant significantly reduced avoidance compared to baseline, VEH, and 0.20 μg/side ($p = 0.011$, $p = 0.014$, $p < 0.001$).

These data suggest that phasic NAcC DA release and VTA eCB signaling are gatekeepers of avoidance. Changes in DA release due to altered CB1 signaling are consistent with a model of presynaptic eCB control of VTA DA neurons [29, 30]. This model recognizes that, although eCBs are mobilized in VTA DA neurons during burst firing, these cells lack CB1 receptors that largely control afferent strength [29, 32, 33] (but see [34]). Thus, rather than direct actions of eCBs on DA neurons, it is hypothesized that eCBs increase firing of these cells via an indirect mechanism involving CB1-mediated inhibition of GABA release [30, 33]. Indeed, inhibitory post-synaptic currents (IPSCs) mediated by $GABA_B$ receptors on VTA DA neurons are inhibited by activation of CB1 receptors located on GABA terminals [31] (Figure 5D), and both DA and non-DA neurons can release the eCB 2-AG [35]. Thus, we hypothesized that intra-VTA rimonabant decreases avoidance through a reduction in the ability of DA neurons to inhibit GABA release. If this is the case, decrements in avoidance following intra-VTA rimonabant should be rescued by artificially causing DA neurons to burst fire with laser stimulation. To test this, TH::Cre+ rats (n = 4) received ChR2 and bilateral optical fibers aimed at the VTA. These fibers were coupled to a guide cannula (also terminating above the VTA) to allow

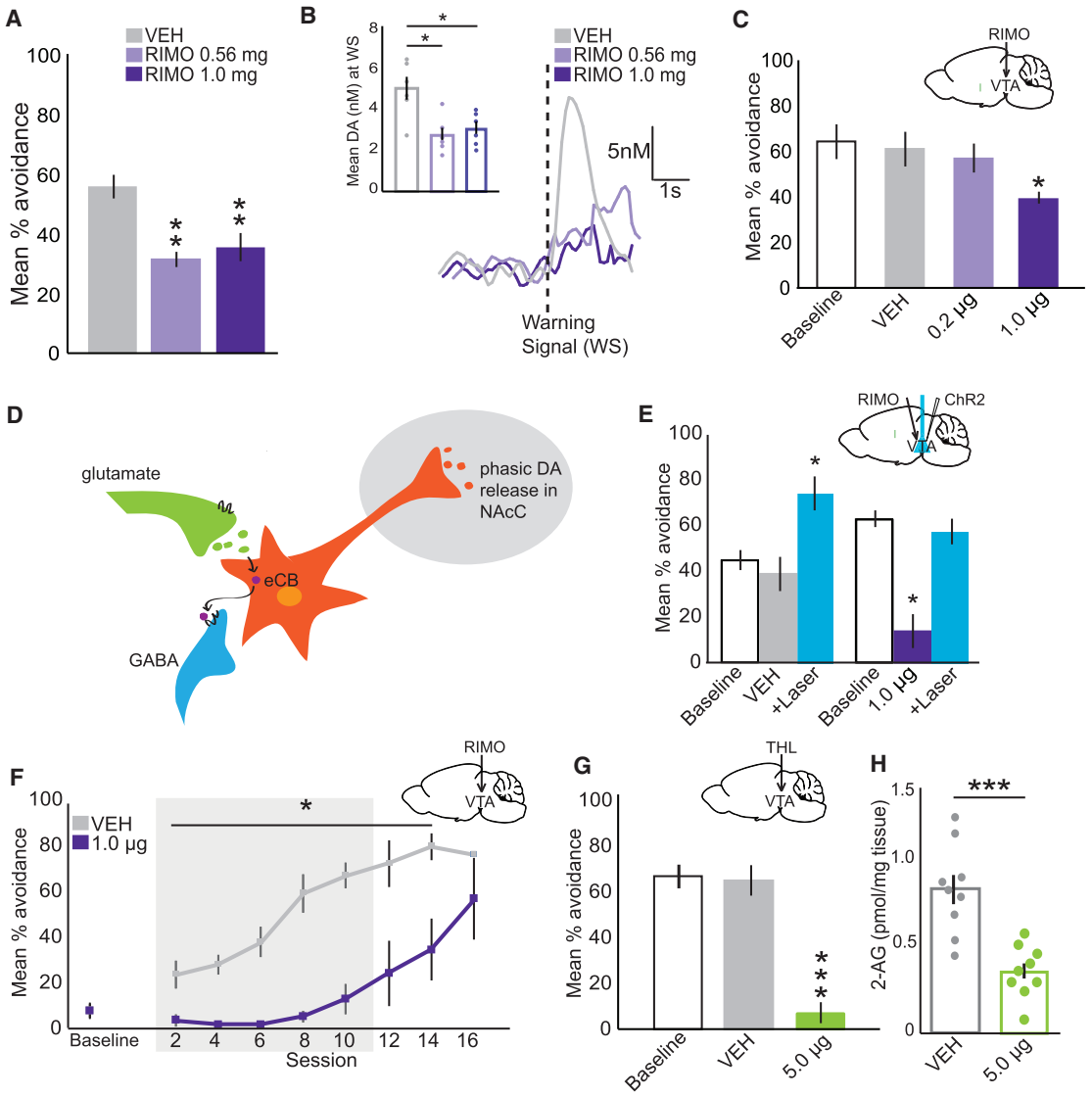

Figure 5. Antagonism of eCB Signaling Attenuates the DA Response to the WS and Active Avoidance

(A) Mean percent avoidance following i.v. VEH or one of two doses of rimonabant (RIMO).

(B) Bar graph showing mean NAcC DA concentration at the WS; dots show data for each rat. Example DA traces showing DAergic response to the WS following VEH or RIMO are shown.

(C) Avoidance at baseline and following intra-VTA VEH or RIMO. Inset illustrates RIMO infusion in VTA.

(D) Diagram illustrating a mechanism by which stimulation of VTA DA cells promotes "on demand" eCB release and CB1-mediated inhibition of GABAergic tone onto DA cells.

(E) Avoidance in rats with bilateral optical fibers coupled to guide cannula in VTA. Avoidance at baseline and following intra-VTA infusion of VEH or RIMO and during trials with VTA laser stimulation ("+LASER") at the WS in conjunction with VEH or RIMO is shown.

(F) Avoidance in rats that received intra-VTA VEH or RIMO before each of the first ten avoidance sessions, after an initial "baseline" session. Rats received no pretreatment prior to sessions 11–16. Data are shown in two-session bins.

(G) Avoidance in rats at baseline or following intra-VTA infusion of VEH or THL.

(H) 2-AG tissue content in rat VTA following intra-VTA infusion of VEH or THL.

Dots represent data for each rat. Error bars are ±SEM; *p ≤ 0.05, **p ≤ 0.01, ***p ≤ 0.001. See also Figures S2 and S3.

for VEH or rimonabant infusion and for delivery of laser light. Rats were trained to ~50% avoidance and then underwent two test sessions, consisting of a 10 min baseline, followed by intra-VTA VEH or rimonabant (1.0 μg/side). Rats then performed for an additional 10 min. For the final 10 min, the laser was turned on and animals performed shock avoidance while receiving laser stimulation at the WS. ANOVA revealed a significant main effect ($F_{5,15}$ = 10.45, p < 0.001; Figure 5E), and post hoc tests confirmed that intra-VTA rimonabant (p = 0.02), but not VEH (p > 0.05), decreased avoidance, and stimulation of DA neurons profoundly increased avoidance following VEH (p = 0.05). Crucially, and in support of our hypothesis, laser stimulation

restored avoidance behavior following the deficits induced by rimonabant ($p = 0.02$).

We also tested the ability of CB1 receptor antagonism to prohibit avoidance learning (n = 6; Figure 5F). Rats were implanted with bilateral cannula aimed at the VTA and, following a single no-drug baseline session, received either intra-VTA vehicle (n = 3) or rimonabant (n = 3; 1 μg/side) prior to each of 10 daily avoidance sessions, followed by six sessions with no drug pretreatment. ANOVA revealed a main effect of trial ($F_{7,28} = 20.198$, $p < 0.001$) and group ($F_{1,4} = 18.206$; $p = 0.013$) with an interaction ($F_{7,28} = 2.692$, $p = 0.029$). Thus, both groups learned to avoid; however, rimonabant pretreatment delayed acquisition of the task. Therefore, intact VTA CB1 signaling is necessary for active avoidance learning. We also tested the ability of VTA DA neuron stimulation to enhance learning of avoidance from the start of training. Interestingly, we found no difference in performance between TH::Cre+ rats (n = 5) and TH::Cre− (n = 5) controls ($p > 0.05$; Figure S2), indicating that in order for laser stimulation to enhance avoidance, animals must have prior knowledge of the cue-response-outcome association (i.e., as seen in animals at ~50% avoidance).

Research suggests that 2-AG is the principal eCB involved in synaptic modification [33, 36] and supports a specific role for VTA 2-AG in cued reinforcement [37]. To determine whether 2-AG mediates avoidance, rats (n = 5) received bilateral VTA guide cannulae, were trained to ~50% avoidance, and underwent three test sessions. The first session served as a baseline. Before session two, rats received intra-VTA VEH, and before the third session, they received intra-VTA infusion of the 2-AG synthesis inhibitor tetrahydrolipstatin (THL; 5.0 μg/side) [31]. THL is a potent inhibitor of 2-AG synthesis via inhibition of the biosynthetic enzyme diacylglycerol lipase. THL attenuated avoidance compared to either baseline or VEH (ANOVA with post hoc analysis; $F_{2,8} = 38.222$, $p < 0.001$; $p = 0.001$; $p = 0.001$; Figure 5G). Mass spectrometry analysis for 2-AG content confirmed that THL attenuated 2-AG tissue levels compared to VEH ($t_{16} = 4.73$, $p < 0.001$; Figure 5H). Further, laser stimulation of VTA DA cells rescued avoidance behavior following intra-VTA THL administration (n = 4; 0.5 μg/side; Figure S4). Importantly, we used a lower dose of THL, still capable of decreasing avoidance, in order to minimize any off-target effects [38]. ANOVA reported a main effect of treatment ($F_{5,15} = 3.450$, $p = 0.026$), and post hoc tests confirmed that THL decreased avoidance ($p = 0.003$) and stimulation enhanced avoidance ($p = 0.000$). VEH did not decrease avoidance ($p > 0.05$), and stimulation robustly enhanced avoidance ($p = 0.014$).

Endocannabinoid Modulation of Inhibition in VTA DA Neurons

To confirm that Cre-recombinase and ChR2 do not alter eCB mobilization in DA neurons, whole-cell electrophysiological recordings were performed (n = 8). As previously reported [29, 31], application of the CB1 receptor antagonist AM251 increased the amplitudes of $GABA_B$ IPSCs via displacement of 2-AG on presynaptic CB1 receptors. As this effect was similar to that reported in wild-type rats [29–31], we conclude that tonic 2-AG function is not altered in TH::Cre+ rats (Figures 6A–6F).

It is established that 2-AG can be released from DA neurons [30, 33]; however, it is unknown whether phasic activation leads to eCB release. Therefore, using the same conditions, we assessed whether phasic optical stimulation (3 s; 6–7 mW) produces eCB-dependent depolarization-induced suppression of inhibition, a well-established physiological marker of eCB function. We predicted that, if eCB release is caused by laser stimulation, there should be a time-locked inhibition of $GABA_B$ currents, mediated by CB1 receptors. Indeed, we found that $GABA_B$ IPSCs were transiently inhibited following ChR2-mediated depolarization and that this inhibition was prevented by AM251 (Figures 6G and 6H). These experiments illustrate "on-demand" release of eCBs during VTA DA neuron depolarization and suggest that this mechanism is most likely recruited during optical depolarization of these cells in our behavioral experiments.

Avoidance Learning, but Not Its Maintenance, Is Controlled by Midbrain eCB Mobilization and Phasic Mesolimbic DA Signaling

Although the experiments described above were performed in animals still learning the task (i.e., at ~50% avoidance), it remains unclear how phasic DA and eCBs are involved in the maintenance of avoidance behavior once it is well learned. TH::Cre+ rats were transduced with ChR2 in the VTA, received bilateral VTA fibers, were trained to ~80% avoidance, and then underwent a single test session consisting of a 15 min baseline and 15 min in which laser stimulation of VTA DA cells was delivered at each WS. Interestingly, stimulation did not increase avoidance ($p > 0.05$; Figure 7A). Thus, at this level of training, DA neuron stimulation is unable to produce even small gains in avoidance. In strong support of this interpretation are findings obtained from another group of rats trained to ~80% avoidance, in which intra-NAcC infusion of SCH (1.0 μg/side) had no effect on performance ($p > 0.05$; Figure 7B). Together, these data suggest that avoidance behavior becomes independent of phasic mesolimbic DA signaling once it is well learned. Notably, in another cohort of rats, intra-VTA infusion of rimonabant (1.0 μg/side) had no effect on avoidance in similarly well-performing animals ($p > 0.05$; Figure 7C), indicating that avoidance also becomes independent of VTA eCB signaling.

To further examine underlying neural substrates, we measured 2-AG function in VTA DA neurons from two additional groups of rats: one performing at ≤50% avoidance (n = 7) and another group performing at ≥80% avoidance (n = 6; Figure 7D). These animals differed only in their performance, not in the number of training sessions they received ($p > 0.05$), and we compared these groups to control animals that did not perform on the task (n = 8; data from Figures 6E and 6F). Interestingly, in contrast to controls untrained in avoidance, $GABA_B$ IPSCs recorded in DA neurons from animals at ≤50% avoidance displayed a smaller increase in amplitude upon AM251 application (Figure 7G; $F_{2,144} = 167.6$, $p < 0.001$; $p = 0.0015$), and more remarkably, rats achieving ≥80% avoidance displayed no measurable increase in $GABA_B$ IPSC amplitude upon AM251 application ($p < 0.001$). These results suggest that eCB mobilization and/or VTA CB1 receptor signaling are progressively blunted as rats master the shock avoidance task.

DISCUSSION

Appetitive cues are accompanied by phasic DA release and drive approach [5, 7–11]. Here, we show that DA signaling is

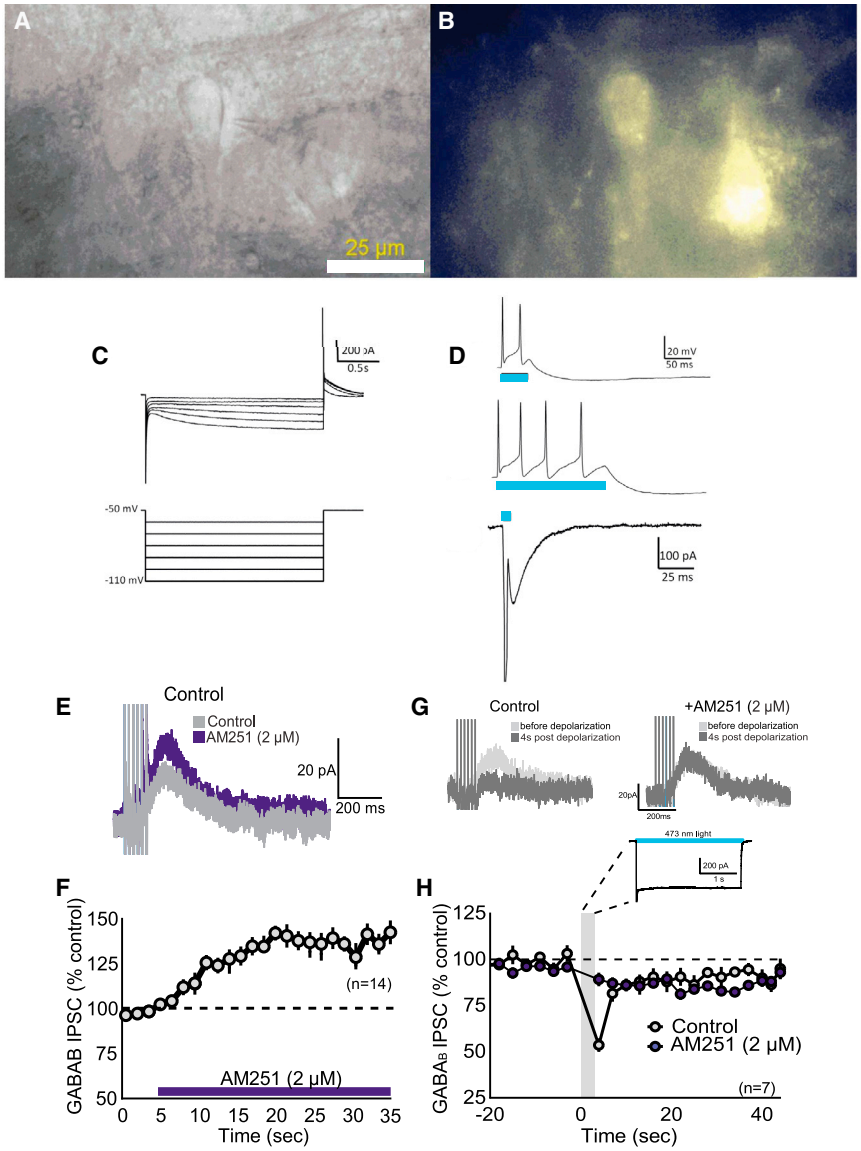

Figure 6. Endocannabinoid Modulation of Synaptic GABA Release in VTA DA Neurons *In Vitro*

(A) Differential interference contrast microscopic image of DA neuron, and adjacent glass-recording pipette, in a VTA brain slice.

(B) Fluorescence image of TH::Cre+ neurons in the VTA expressing ChR2 and eYFP.

(C) Voltage steps (bottom) used to measure input resistance and determine the presence of hyperpolarization-activated inward current (top) found in most lateral VTA DA neurons.

(D) Response of DA neuron recorded in current clamp (membrane potential ~−65 mV) to 473 nm laser light (blue line) applied for 50 ms (top trace) and 200 ms (middle trace). Bottom trace shows response to 5 ms light application during voltage clamp recording of the same neuron (Vhold = −70 mV).

(E) Mean waveforms showing effect of AM251 on $GABA_B$ IPSCs from a representative VTA DA neuron.

(F) Mean time course (±95% confidence interval [CI]) of antagonism of CB1 receptors with AM251 on $GABA_B$ IPSCs elicited in VTA DA neurons with five-pulse, 50 Hz electrical stimulation (n = 14 cells). Increased IPSC amplitude following AM251 indicates antagonism of inhibitory 2-AG tone.

(G) Waveforms from a ChR2-expressing VTA DA neuron showing $GABA_B$ IPSCs evoked using five-pulse, 50 Hz electrical stimulation, before and 4 s after depolarization by light. Note the inhibition of the $GABA_B$ IPSC response under control conditions and the absence of inhibition following AM251.

(H) Mean time course of $GABA_B$ IPSCs evoked every 4 s and effect of a 3 s depolarization evoked by light activation of ChR2 (inset and gray vertical bar).

Error bars are ±SEM.

also essential for behavior guided by negative reinforcement. With precise temporal control afforded by optogenetics, we show that activation of VTA DA neurons at the presentation of a WS enhances active avoidance, whereas inhibition of DA cells attenuates it. We demonstrate that this effect is DA dependent, as gains in avoidance are abolished by simultaneous antagonism of D1, but not D2, receptors. Moreover, with the use of terminal stimulation, we demonstrate that NAcC, but not PFC, DA release causes avoidance. These findings expand our previous FSCV data [8], which showed a positive correlation between DA release and avoidance and decreased DA release prior to an escape response [8]. Interestingly, mimicking such reductions with a D1 receptor antagonist reverses the response ratio to favor escape over avoidance and establishes a causal role for reduced DA signaling in the failure to successfully avoid shock.

The current data align with Mowrer's two-process theory of avoidance [13], which postulates that avoidance involves two processes: an initial classically conditioned response to the aversive cue and subsequent acquisition of the operant response, reinforced by cue removal (but see [39, 40]). Prior to escape, the WS is theorized to convey an impending aversive stimulus and DA release is reduced [6, 8, 41, 42]. The initial conditioned fear response is a species-specific defensive behavior (freezing in rodents) that interferes with avoidance [43]. Unquestionably, escape predominates during early performance, suggesting an initial stage of learning marked by cue-induced freezing. However, as training progresses, animals learn the operant sequence. Thus, when successful avoidance responses emerge, the WS most likely conveys safety, resulting in avoidance probably through dopaminergic learning mechanisms [12, 44]. Taken together, our data provide a neurobiological substrate for two-process avoidance learning and strong evidence that environmental cues predicting avoidable aversive stimuli enhance DA release to cause avoidance, whereas stimuli predicting unavoidable footshock inhibit both processes.

Our laboratory and others have previously shown that cues associated with unavoidable footshock are accompanied by

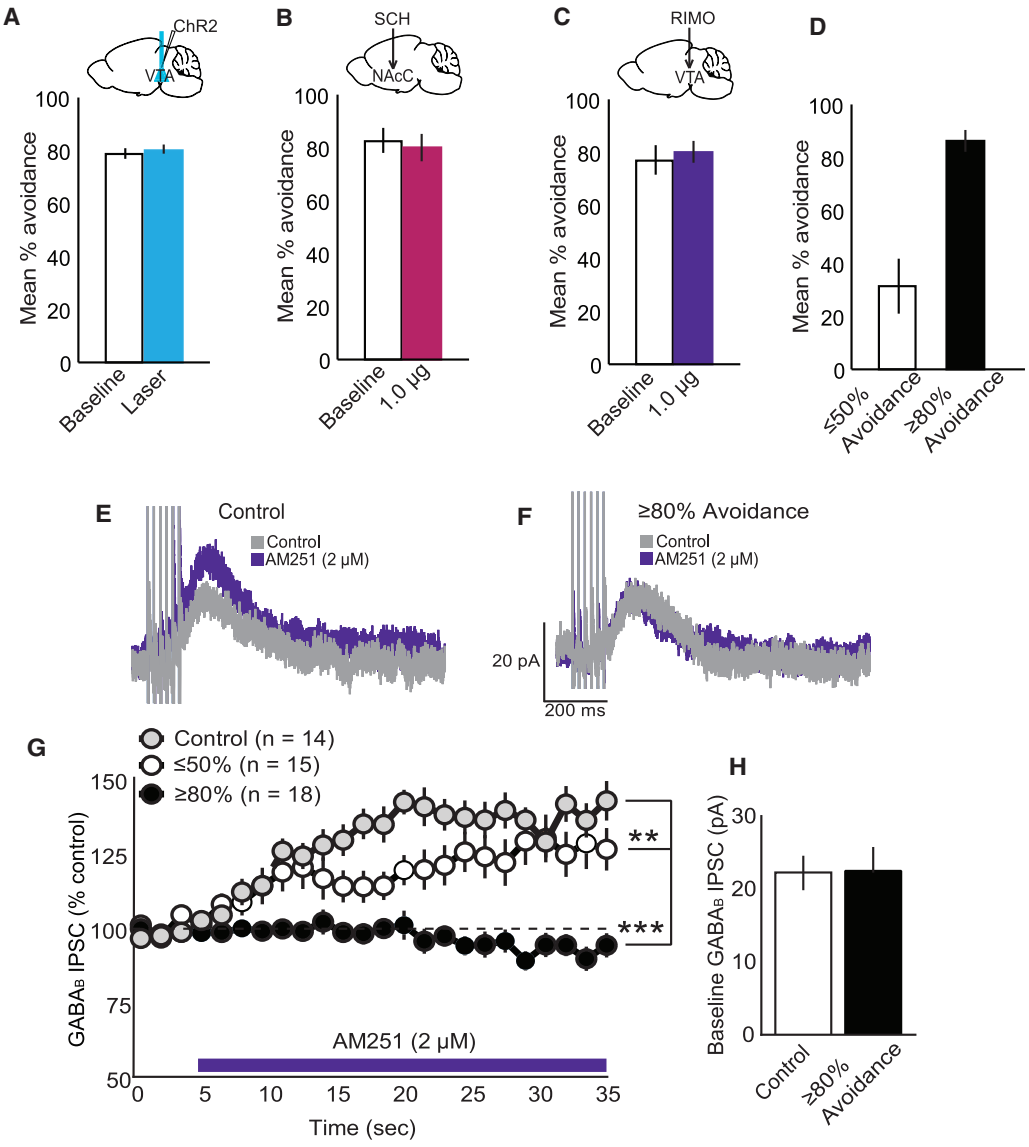

Figure 7. Active Avoidance Learning, but Not Maintenance, Is Controlled by Midbrain eCBs and Phasic Mesolimbic DA Signaling

(A) Mean percent avoidance at baseline and during laser stimulation of VTA DA cells at the WS. Note that at baseline, rats are avoiding on ~80% of trials.

(B) Mean avoidance at baseline and following intra-NAcC infusion of SCH23390 (SCH).

(C) Mean avoidance at baseline and following intra-VTA infusion of rimonabant (RIMO).

(D) Mean avoidance of two groups of rats. One group reached ~50% avoidance, whereas the other group performed at ~80% avoidance. Following behavior, animals were euthanized and their brains were used to assess eCB modulation of synaptic GABA release onto VTA DA neurons (E–H).

(E) Waveforms showing effect of AM251 on electrically evoked $GABA_B$ IPSCs (five pulses, 50 Hz) from a single VTA DA neuron obtained from a control animal (data also shown in Figure 6, shown here again for comparison).

(F) Waveforms showing the effect of AM251 on $GABA_B$ IPSCs in a DA neuron obtained from a rat that had achieved ≥80% avoidance.

(G) Mean time course of AM251 on $GABA_B$ IPSCs elicited in VTA DA neurons obtained from control rats (data also shown in Figure 6) and rats that achieved ≤50% and ≥80% avoidance behavior.

(H) Data demonstrating that baseline $GABA_B$ IPSCs were not affected by avoidance training.

Error bars are ±SEM; **p ≤ 0.01, ***p ≤ 0.001.

pauses in phasic DA release and freezing behavior [6, 8]. As freezing is extinguished, DA also returns to baseline, and with laser stimulation, we reverse cue-evoked pauses in mesolimbic DA signaling and diminish conditioned freezing [45]. This effect was enduring, as animals continued to show attenuated conditioned freezing the next day in the absence of laser. Thus, just as the transition from escape to avoidance requires cue-induced DAergic activation, enhancing DA release decreases cue-induced freezing and expedites the extinction of conditioned fear. However, the question of whether laser stimulation produces these effects by blocking the expression of conditioned freezing, enhancing learning of the new cue

contingency, or a combination of these mechanisms remains unknown.

Our results show that DAergic responses to a cue predicting avoidable negative stimuli mirror the DA response to cues that predict positive/rewarding stimuli. Appetitive cue-evoked DA release is under the control of midbrain eCBs [37], and CB1 receptor signaling mediates DAergic positive reinforcement mechanisms [46, 47]. Here, we present evidence that eCBs similarly regulate the DAergic response to aversive cues. Indeed, rimonabant blocked both avoidance and WS-evoked NAcC DA release. Moreover, inhibition of 2-AG synthesis robustly blocked avoidance. These data align with a mechanism in which stimulus-induced activation of DA neurons leads to enhanced mobilization of 2-AG [29, 30] and inhibition of GABA input to VTA DA neurons [29–31], promoting additional WS-induced phasic DA release in the NacC, thus permitting avoidance to dominate the animal's behavioral repertoire. Here, we provide *ex vivo* evidence that phasic activation of DA cells releases 2-AG to transiently inhibit release of GABA onto DA neurons, thereby most likely prolonging the depolarizing response. Of course, the involvement of this mechanism in cue-induced DA neuron activation and eCB release remains speculative.

Interestingly, once rats mastered avoidance responding ($\geq$80% avoidance), neither NAcC D1 nor VTA CB1 receptor antagonism disrupted avoidance—manipulations that robustly decreased avoidance in animals learning the task ($\sim$50% avoidance). This most likely indicates that well-learned avoidance behavior is maintained by other neural systems. One possibility is that, as rats learn, avoidance responding becomes habitual and is sustained by nigrostriatal DA systems [48, 49].

Our data also show that avoidance learning is coupled with a decrease in VTA eCB dynamics. CB1 antagonism results in robust increases in $GABA_B$ IPSCs in control rats; however, CB1 antagonism no longer increases GABA release onto VTA DA cells in rats performing at $\geq$80% avoidance and is significantly impaired in rats performing at $\leq$50%. This suggests that 2-AG signaling is important during acquisition, but not after avoidance is well learned. Thus, avoidance learning most likely coincides with either decreased 2-AG mobilization or a reduction in VTA CB1 receptor function or number. Although others have demonstrated experience-dependent CB1 receptor downregulation or alterations in eCB levels [50–52], our data expand these findings by showing that learning, and not just passive exposure to a stimulus (e.g., drugs or stress), fundamentally changes eCB signaling. Indeed, this adaptation is unlikely to be due to stressor exposure as the $\leq$50% and $\geq$80% avoidance groups had similar amounts of training, and animals in the $\geq$80% group receive the fewest number of shocks but display the largest effect on 2-AG mobilization.

Our findings define a unique role for DA in the response to aversive stimuli and indicate that cue-induced NAcC DA signaling promotes active over passive defensive behaviors. It is posited that freezing is under the control of the amygdala and the periaqueductal gray, whereas active avoidance is mediated by the basal amygdala and NAc [53]. Therefore, optical stimulation, and resultant NAcC DA release, may preferentially activate avoidance over neural systems related to freezing to promote alternative (perhaps more adaptive) defensive behaviors. It is noteworthy that DAergic activation resulted in a lasting attenuation of conditioned fear, suggesting that DA signaling may provide a therapeutic target for psychological disorders related to defensive behavior. For example, post-traumatic stress disorder (PTSD) is characterized by pathological avoidance of stressful environments. Conversely, depression is marked by a lack of avoidance resulting in rumination and helplessness. Indeed, preclinical evidence indicates that cannabinoids may provide relief from symptoms of depression [54], and cannabinoid drugs are currently in clinical trials for the treatment of PTSD [55]. Thus, the ability of these pharmacotherapies to enhance phasic DAergic activity may underlie their efficacy, through alteration of active versus passive defense behaviors and/or by way of enhanced extinction of conditioned responses.

STAR★METHODS

Detailed methods are provided in the online version of this paper and include the following:

- KEY RESOURCES TABLE
- CONTACT FOR REAGENT AND RESOURCE SHARING
- EXPERIMENTAL MODEL AND SUBJECT DETAILS
  - Subjects
  - Optogenetic virus injection and optical fiber implantation
  - Voltammetric electrode implantation
  - Cannula implantation
  - IV catheter implantation
- METHOD DETAILS
  - Avoidance task
  - Optogenetic manipulation of avoidance
  - Pharmacological manipulation of avoidance
  - *In vivo* voltammetry
  - Drugs for *in vivo* use
  - Variable time out (VTO) task
  - Fear conditioning
  - Locomotor testing
  - *Ex vivo* voltammetry
  - Slice electrophysiology
  - LC-MS/MS
  - Histology
- QUANTIFICATION AND STATISTICAL ANALYSIS

SUPPLEMENTAL INFORMATION

Supplemental Information includes six figures and one video and can be found with this article online at https://doi.org/10.1016/j.cub.2018.03.037.

ACKNOWLEDGMENTS

The authors would like to thank Dr. Yolanda Mateo, Dr. Margaret Davis, Iness Gildish, Victoria Ayvazian, Vivian Chioma, and Dr. James Irving for their expert technical assistance and Dr. Natalie Zlebnik and Dr. Dan Covey for helpful discussion and critical review of this manuscript. We would also like to thank Dr. Patricia Janak as well as Dr. Geoff Schoenbaum and his laboratory for invaluable feedback. This research was supported by the US National Institute on Drug Abuse (grant DA022340) awarded to J.F.C. and funding from the National Institute on Drug Abuse Intramural Research Program (C.R.L. and D.I.D.).

AUTHOR CONTRIBUTIONS

Conceptualization and Methodology, J.M.W., E.B.O., C.R.L., and J.F.C.; Investigation and Formal Analysis, J.M.W., E.B.O., W.N.G., A.B.C., H.M.D., U.G., R.J.B., and D.I.D.; Resources, G.D.S., K.D., B.N.M., S.P., and C.R.L.; Writing, J.M.W., C.R.L., and J.F.C.; Funding Acquisition, C.R.L. and J.F.C.

DECLARATION OF INTERESTS

The authors declare no competing interests.

Received: February 7, 2018
Revised: March 12, 2018
Accepted: March 15, 2018
Published: April 19, 2018

REFERENCES

1. Schultz, W., Dayan, P., and Montague, P.R. (1997). A neural substrate of prediction and reward. Science *275*, 1593–1599.
2. Swanson, L.W. (1982). The projections of the ventral tegmental area and adjacent regions: a combined fluorescent retrograde tracer and immunofluorescence study in the rat. Brain Res. Bull. *9*, 321–353.
3. Grace, A.A. (1991). Phasic versus tonic dopamine release and the modulation of dopamine system responsivity: a hypothesis for the etiology of schizophrenia. Neuroscience *41*, 1–24.
4. Mirenowicz, J., and Schultz, W. (1996). Preferential activation of midbrain dopamine neurons by appetitive rather than aversive stimuli. Nature *379*, 449–451.
5. Roitman, M.F., Stuber, G.D., Phillips, P.E., Wightman, R.M., and Carelli, R.M. (2004). Dopamine operates as a subsecond modulator of food seeking. J. Neurosci. *24*, 1265–1271.
6. Badrinarayan, A., Wescott, S.A., Vander Weele, C.M., Saunders, B.T., Couturier, B.E., Maren, S., and Aragona, B.J. (2012). Aversive stimuli differentially modulate real-time dopamine transmission dynamics within the nucleus accumbens core and shell. J. Neurosci. *32*, 15779–15790.
7. Matsumoto, M., and Hikosaka, O. (2009). Two types of dopamine neuron distinctly convey positive and negative motivational signals. Nature *459*, 837–841.
8. Oleson, E.B., Gentry, R.N., Chioma, V.C., and Cheer, J.F. (2012). Subsecond dopamine release in the nucleus accumbens predicts conditioned punishment and its successful avoidance. J. Neurosci. *32*, 14804–14808.
9. Romo, R., and Schultz, W. (1990). Dopamine neurons of the monkey midbrain: contingencies of responses to active touch during self-initiated arm movements. J. Neurophysiol. *63*, 592–606.
10. Saddoris, M.P., Cacciapaglia, F., Wightman, R.M., and Carelli, R.M. (2015). Differential dopamine release dynamics in the nucleus accumbens core and shell reveal complementary signals for error prediction and incentive motivation. J. Neurosci. *35*, 11572–11582.
11. Steinberg, E.E., Keiflin, R., Boivin, J.R., Witten, I.B., Deisseroth, K., and Janak, P.H. (2013). A causal link between prediction errors, dopamine neurons and learning. Nat. Neurosci. *16*, 966–973.
12. Lloyd, K., and Dayan, P. (2016). Safety out of control: dopamine and defence. Behav. Brain Funct. *12*, 15.
13. Mowrer, O.H. (1947). On the dual nature of learning—a re-interpretation of" conditioning" and" problem-solving. Harv. Educ. Rev. *17*, 102–148.
14. Melis, M., and Pistis, M. (2012). Hub and switches: endocannabinoid signalling in midbrain dopamine neurons. Philos. Trans. R. Soc. Lond. B Biol. Sci. *367*, 3276–3285.
15. Hamid, A.A., Pettibone, J.R., Mabrouk, O.S., Hetrick, V.L., Schmidt, R., Vander Weele, C.M., Kennedy, R.T., Aragona, B.J., and Berke, J.D. (2016). Mesolimbic dopamine signals the value of work. Nat. Neurosci. *19*, 117–126.
16. Ilango, A., Kesner, A.J., Keller, K.L., Stuber, G.D., Bonci, A., and Ikemoto, S. (2014). Similar roles of substantia nigra and ventral tegmental dopamine neurons in reward and aversion. J. Neurosci. *34*, 817–822.
17. McCutcheon, J.E., Cone, J.J., Sinon, C.G., Fortin, S.M., Kantak, P.A., Witten, I.B., Deisseroth, K., Stuber, G.D., and Roitman, M.F. (2014). Optical suppression of drug-evoked phasic dopamine release. Front. Neural Circuits *8*, 114.
18. Porrino, L.J., and Goldman-Rakic, P.S. (1982). Brainstem innervation of prefrontal and anterior cingulate cortex in the rhesus monkey revealed by retrograde transport of HRP. J. Comp. Neurol. *205*, 63–76.
19. Naneix, F., Marchand, A.R., Di Scala, G., Pape, J.-R., and Coutureau, E. (2009). A role for medial prefrontal dopaminergic innervation in instrumental conditioning. J. Neurosci. *29*, 6599–6606.
20. Schultz, W., Apicella, P., and Ljungberg, T. (1993). Responses of monkey dopamine neurons to reward and conditioned stimuli during successive steps of learning a delayed response task. J. Neurosci. *13*, 900–913.
21. Lacroix, L., Broersen, L.M., Weiner, I., and Feldon, J. (1998). The effects of excitotoxic lesion of the medial prefrontal cortex on latent inhibition, prepulse inhibition, food hoarding, elevated plus maze, active avoidance and locomotor activity in the rat. Neuroscience *84*, 431–442.
22. Dreyer, J.K., Herrik, K.F., Berg, R.W., and Hounsgaard, J.D. (2010). Influence of phasic and tonic dopamine release on receptor activation. J. Neurosci. *30*, 14273–14283.
23. Cooper, B.R., Howard, J.L., Grant, L.D., Smith, R.D., and Breese, G.R. (1974). Alteration of avoidance and ingestive behavior after destruction of central catecholamine pathways with 6-hydroxydopamine. Pharmacol. Biochem. Behav. *2*, 639–649.
24. McCullough, L.D., Sokolowski, J.D., and Salamone, J.D. (1993). A neurochemical and behavioral investigation of the involvement of nucleus accumbens dopamine in instrumental avoidance. Neuroscience *52*, 919–925.
25. Ishikawa, A., Ambroggi, F., Nicola, S.M., and Fields, H.L. (2008). Contributions of the amygdala and medial prefrontal cortex to incentive cue responding. Neuroscience *155*, 573–584.
26. Shull, R.L., Gaynor, S.T., and Grimes, J.A. (2001). Response rate viewed as engagement bouts: effects of relative reinforcement and schedule type. J. Exp. Anal. Behav. *75*, 247–274.
27. Wenzel, J.M., and Cheer, J.F. (2014). Endocannabinoid-dependent modulation of phasic dopamine signaling encodes external and internal reward-predictive cues. Front. Psychiatry *5*, 118.
28. Marsicano, G., Wotjak, C.T., Azad, S.C., Bisogno, T., Rammes, G., Cascio, M.G., Hermann, H., Tang, J., Hofmann, C., Zieglgänsberger, W., et al. (2002). The endogenous cannabinoid system controls extinction of aversive memories. Nature *418*, 530–534.
29. Lupica, C.R., and Riegel, A.C. (2005). Endocannabinoid release from midbrain dopamine neurons: a potential substrate for cannabinoid receptor antagonist treatment of addiction. Neuropharmacology *48*, 1105–1116.
30. Riegel, A.C., and Lupica, C.R. (2004). Independent presynaptic and postsynaptic mechanisms regulate endocannabinoid signaling at multiple synapses in the ventral tegmental area. J. Neurosci. *24*, 11070–11078.
31. Wang, H., Treadway, T., Covey, D.P., Cheer, J.F., and Lupica, C.R. (2015). Cocaine-induced endocannabinoid mobilization in the ventral tegmental area. Cell Rep. *12*, 1997–2008.
32. Herkenham, M., Lynn, A.B., Johnson, M.R., Melvin, L.S., de Costa, B.R., and Rice, K.C. (1991). Characterization and localization of cannabinoid receptors in rat brain: a quantitative in vitro autoradiographic study. J. Neurosci. *11*, 563–583.
33. Melis, M., Pistis, M., Perra, S., Muntoni, A.L., Pillolla, G., and Gessa, G.L. (2004). Endocannabinoids mediate presynaptic inhibition of glutamatergic transmission in rat ventral tegmental area dopamine neurons through activation of CB1 receptors. J. Neurosci. *24*, 53–62.
34. Zhang, H.Y., Gao, M., Shen, H., Bi, G.H., Yang, H.J., Liu, Q.R., Wu, J., Gardner, E.L., Bonci, A., and Xi, Z.X. (2016). Expression of functional

cannabinoid CB2 receptor in VTA dopamine neurons in rats. Addict. Biol. *22*, 752–765.

35. Mátyás, F., Urbán, G.M., Watanabe, M., Mackie, K., Zimmer, A., Freund, T.F., and Katona, I. (2008). Identification of the sites of 2-arachidonoylglycerol synthesis and action imply retrograde endocannabinoid signaling at both GABAergic and glutamatergic synapses in the ventral tegmental area. Neuropharmacology *54*, 95–107.
36. Tanimura, A., Yamazaki, M., Hashimotodani, Y., Uchigashima, M., Kawata, S., Abe, M., Kita, Y., Hashimoto, K., Shimizu, T., Watanabe, M., et al. (2010). The endocannabinoid 2-arachidonoylglycerol produced by diacylglycerol lipase alpha mediates retrograde suppression of synaptic transmission. Neuron *65*, 320–327.
37. Oleson, E.B., Beckert, M.V., Morra, J.T., Lansink, C.S., Cachope, R., Abdullah, R.A., Loriaux, A.L., Schetters, D., Pattij, T., Roitman, M.F., et al. (2012). Endocannabinoids shape accumbal encoding of cue-motivated behavior via CB1 receptor activation in the ventral tegmentum. Neuron *73*, 360–373.
38. Ortar, G., Bisogno, T., Ligresti, A., Morera, E., Nalli, M., and Di Marzo, V. (2008). Tetrahydrolipstatin analogues as modulators of endocannabinoid 2-arachidonoylglycerol metabolism. J. Med. Chem. *51*, 6970–6979.
39. Fernando, A.B.P., Urcelay, G.P., Mar, A.C., Dickinson, A., and Robbins, T.W. (2014). Safety signals as instrumental reinforcers during free-operant avoidance. Learn. Mem. *21*, 488–497.
40. Lovibond, P.F., Saunders, J.C., Weidemann, G., and Mitchell, C.J. (2008). Evidence for expectancy as a mediator of avoidance and anxiety in a laboratory model of human avoidance learning. Q. J. Exp. Psychol. *61*, 1199–1216.
41. Gentry, R.N., Lee, B., and Roesch, M.R. (2016). Phasic dopamine release in the rat nucleus accumbens predicts approach and avoidance performance. Nat. Commun. *7*, 13154.
42. Wheeler, D.S., Robble, M.A., Hebron, E.M., Dupont, M.J., Ebben, A.L., and Wheeler, R.A. (2015). Drug predictive cues activate aversion-sensitive striatal neurons that encode drug seeking. J. Neurosci. *35*, 7215–7225.
43. Bolles, R.C. (1969). Avoidance and escape learning: simultaneous acquisition of different responses. J. Comp. Physiol. Psychol. *68*, 355–358.
44. Maia, T.V. (2010). Two-factor theory, the actor-critic model, and conditioned avoidance. Learn. Behav. *38*, 50–67.
45. Bouchet, C.A., Miner, M.A., Loetz, E.C., Rosberg, A.J., Hake, H.S., Farmer, C.E., Ostrovskyy, M., Gray, N., and Greenwod, B.N. (2018). Activation of nigrostriatal dopamine neurons during fear extinction prevents the renewal of fear. Neuropsychopharmacology *43*, 665–672.
46. Cheer, J.F., Wassum, K.M., Sombers, L.A., Heien, M.L.A.V., Ariansen, J.L., Aragona, B.J., Phillips, P.E., and Wightman, R.M. (2007). Phasic dopamine release evoked by abused substances requires cannabinoid receptor activation. J. Neurosci. *27*, 791–795.
47. Hernandez, G., Bernstein, D., Schoenbaum, G., and Cheer, J.F. (2011). Contrasting effects of lithium chloride and CB1 receptor blockade on enduring changes in the valuation of reward. Front. Behav. Neurosci. *5*, 53.
48. Everitt, B.J., and Robbins, T.W. (2013). From the ventral to the dorsal striatum: devolving views of their roles in drug addiction. Neurosci. Biobehav. Rev. *37* (9 Pt A), 1946–1954.
49. Graybiel, A.M. (2008). Habits, rituals, and the evaluative brain. Annu. Rev. Neurosci. *31*, 359–387.
50. Di Marzo, V., Berrendero, F., Bisogno, T., González, S., Cavaliere, P., Romero, J., Cebeira, M., Ramos, J.A., and Fernández-Ruiz, J.J. (2000). Enhancement of anandamide formation in the limbic forebrain and reduction of endocannabinoid contents in the striatum of delta9-tetrahydrocannabinol-tolerant rats. J. Neurochem. *74*, 1627–1635.
51. Morena, M., Patel, S., Bains, J.S., and Hill, M.N. (2016). Neurobiological interactions between stress and the endocannabinoid system. Neuropsychopharmacology *41*, 80–102.
52. Wamsteeker, J.I., Kuzmiski, J.B., and Bains, J.S. (2010). Repeated stress impairs endocannabinoid signaling in the paraventricular nucleus of the hypothalamus. J. Neurosci. *30*, 11188–11196.
53. LeDoux, J.E., Moscarello, J., Sears, R., and Campese, V. (2017). The birth, death and resurrection of avoidance: a reconceptualization of a troubled paradigm. Mol. Psychiatry *22*, 24–36.
54. Kruk-Slomka, M., Michalak, A., and Biala, G. (2015). Antidepressant-like effects of the cannabinoid receptor ligands in the forced swimming test in mice: mechanism of action and possible interactions with cholinergic system. Behav. Brain Res. *284*, 24–36.
55. Rabinak, C.A. (2017). Cannabinoid control of fear extinction neural circuits in post-traumatic stress disorder. https://clinicaltrials.gov/ct2/show/NCT02069366.
56. Clark, J.J., Sandberg, S.G., Wanat, M.J., Gan, J.O., Horne, E.A., Hart, A.S., Akers, C.A., Parker, J.G., Willuhn, I., Martinez, V., et al. (2010). Chronic microsensors for longitudinal, subsecond dopamine detection in behaving animals. Nat. Methods *7*, 126–129.
57. Heien, M.L.A.V., Phillips, P.E.M., Stuber, G.D., Seipel, A.T., and Wightman, R.M. (2003). Overoxidation of carbon-fiber microelectrodes enhances dopamine adsorption and increases sensitivity. Analyst (Lond.) *128*, 1413–1419.
58. Jennings, J.H., Sparta, D.R., Stamatakis, A.M., Ung, R.L., Pleil, K.E., Kash, T.L., and Stuber, G.D. (2013). Distinct extended amygdala circuits for divergent motivational states. Nature *496*, 224–228.
59. Nowend, K.L., Arizzi, M., Carlson, B.B., and Salamone, J.D. (2001). D1 or D2 antagonism in nucleus accumbens core or dorsomedial shell suppresses lever pressing for food but leads to compensatory increases in chow consumption. Pharmacol. Biochem. Behav. *69*, 373–382.
60. Saunders, B.T., and Robinson, T.E. (2012). The role of dopamine in the accumbens core in the expression of Pavlovian-conditioned responses. Eur. J. Neurosci. *36*, 2521–2532.
61. Yun, I.A., Nicola, S.M., and Fields, H.L. (2004). Contrasting effects of dopamine and glutamate receptor antagonist injection in the nucleus accumbens suggest a neural mechanism underlying cue-evoked goal-directed behavior. Eur. J. Neurosci. *20*, 249–263.
62. Hernandez, G., and Cheer, J.F. (2011). Extinction learning of rewards in the rat: is there a role for CB1 receptors? Psychopharmacology (Berl.) *217*, 189–197.
63. Hernandez, G., and Cheer, J.F. (2012). Effect of CB1 receptor blockade on food-reinforced responding and associated nucleus accumbens neuronal activity in rats. J. Neurosci. *32*, 11467–11477.
64. Hernandez, G., Oleson, E.B., Gentry, R.N., Abbas, Z., Bernstein, D.L., Arvanitogiannis, A., and Cheer, J.F. (2014). Endocannabinoids promote cocaine-induced impulsivity and its rapid dopaminergic correlates. Biol. Psychiatry *75*, 487–498.
65. Morra, J.T., Glick, S.D., and Cheer, J.F. (2010). Neural encoding of psychomotor activation in the nucleus accumbens core, but not the shell, requires cannabinoid receptor signaling. J. Neurosci. *30*, 5102–5107.
66. Gregg, L.C., Jung, K.M., Spradley, J.M., Nyilas, R., Suplita, R.L., 2nd, Zimmer, A., Watanabe, M., Mackie, K., Katona, I., Piomelli, D., and Hohmann, A.G. (2012). Activation of type 5 metabotropic glutamate receptors and diacylglycerol lipase-α initiates 2-arachidonoylglycerol formation and endocannabinoid-mediated analgesia. J. Neurosci. *32*, 9457–9468.
67. Buchta, W.C., Mahler, S.V., Harlan, B., Aston-Jones, G.S., and Riegel, A.C. (2017). Dopamine terminals from the ventral tegmental area gate intrinsic inhibition in the prefrontal cortex. Physiol. Rep. *5*, e13198.
68. Witten, I.B., Steinberg, E.E., Lee, S.Y., Davidson, T.J., Zalocusky, K.A., Brodsky, M., Yizhar, O., Cho, S.L., Gong, S., Ramakrishnan, C., et al. (2011). Recombinase-driver rat lines: tools, techniques, and optogenetic application to dopamine-mediated reinforcement. Neuron *72*, 721–733.

STAR★METHODS

KEY RESOURCES TABLE

REAGENT or RESOURCE	SOURCE	IDENTIFIER
Antibodies		
TH primary antibody (TH-mouse)	Frontier Institute	N/A
GFP primary antibody (GFP-chicken)	Aves Labs	GFP-1020
GFP secondary antibody (donkey anti-chicken: Alexa Fluor 594 AffiniPure Donkey Anti-Chicken IgY (IgG) (H+L)	Jackson Laboratories	703-585-155
TH secondary antibody (donkey anti-mouse: AffiniPure Donkey Anti-Mouse IgG (H+L))	Jackson Laboratories	715-005-151
Bacterial and Virus Strains		
AAV5-EF1a-DIO-hChR2(h134r)-EYFP	UNC Vector Core	N/A
AAV-EF1a-DIO-eNpHR3.0-EYFP	UNC Vector Core	N/A
Chemicals, Peptides, and Recombinant Proteins		
SCH23390	Sigma-Aldrich	125941-87-9
Eticlopride	Sigma-Aldrich	97612-24-3
Rimonabant	NIDA Drug Supply Program	NOCD-082
AM251	Tocris	Cat. No. 1117
Tetrahydrolipstatin	Tocris	Cat. No. 3540
Experimental Models: Organisms/Strains		
Rat: TH::Cre on Long-Evans background	Karl Diesseroth	N/A
Software and Algorithms		
SPSS	IBM	N/A
Prism	Graphpad Software	N/A
Tarheel CV and HDCV analysis	Open source (UNC)	N/A
WinLTP	WinLTP	N/A

CONTACT FOR REAGENT AND RESOURCE SHARING

Further information and requests for reagents and resources should be directed to and will be fulfilled by the Lead Contact, Dr. Joseph F. Cheer (jcheer@som.umaryland.edu).

EXPERIMENTAL MODEL AND SUBJECT DETAILS

Subjects

Subjects were male transgenic rats (Long-Evans) expressing Cre-recombinase under the control of the tyrosine hydroxylase promoter (heterozygous, TH::Cre+; n = 44) and wild-type litter mates (TH::Cre-; n = 66). Rats were bred on-site and were group-housed to 275–350 g when they received surgery and were singly housed thereafter in plastic tubs in a 22°C vivarium on a 12-hour light/dark cycle (lights on at 0800 hours). Subjects had *ad libitum* access to food (Purina Rat Chow) and water unless otherwise stated. All methods and procedures were conducted in strict adherence to the *NIH Guide for the Care and Use of Laboratory Animals* and were approved by the University of Maryland School of Medicine Institutional Animal Care and Use Committee. Our TH::Cre rat colony could not have been established without Dr. Karl Deisseroth's assistance and for his donation of our founder animals.

Optogenetic virus injection and optical fiber implantation

The Cre-dependent viruses AAV5-EF1a-DIO-hChR2(h134r)-EYFP (ChR2), and AAV-EF1a-DIO-eNpHR3.0-EYFP (NpHR) (titer, 1.5–4 × 1012 particles/mL) were purchased from the University of North Carolina Vector Core.

Four small holes were drilled over the VTA at the following coordinates: −5.4 and −6.4 AP; ± 0.7 ML. A 5μL Hamilton syringe in a motorized syringe pump was used to deliver 0.5 μL of virus (0.05 μL per minute) at two depths in each hole (−8.4 and −7.4 DV, from brain surface). The needle was left in place for an additional 5min following injection. Bilateral optical fibers were targeted above the VTA (−5.8 AP; +/−0.7 ML; −7.7 DV), the NAcC (+1.7 AP; +/−1.7 ML; −6.6 DV), or the PFC (+3.2 AP; +/−0.5 ML; −3.5 DV). Fibers were made in-house with optical fiber (HUV 200/230 T 48, Ceramoptec) and a zirconia ferrule (FZ1-LC-235, Kientec Systems).

Voltammetric electrode implantation

Rats received chronic electrodes [8, 56] aimed at the NAcC (+1.3 AP; +1.4 ML; −6.9 DV). A bipolar stimulating electrode (Plastics One) was aimed at the ipsilateral medial forebrain bundle (−2.8 AP; +1.7 ML; −8.8 DV), and an Ag/AgCl reference electrode was placed in the contralateral hemisphere. A triangular voltammetric input waveform (initial ramp, −0.4–1.3V, 400V/s) [57] was applied to the working electrode at 10Hz, while subsecond DA release was monitored. Electrical stimulation (60 pulses, 60Hz, 300 μA, 2ms/phase) was applied to the stimulating electrode via a constant-current isolator (A-M Systems). The working electrode was moved ventrally until electrically evoked DA release was detected, dental cement and screws were use to secure the assembly. Subjects were allowed 3 weeks to recover.

Cannula implantation

Bilateral guide cannula (Plastics One, 26 GA) for IC drug infusion were implanted at the following coordinates: VTA, −5.8 AP, +/− 0.7 ML, −5.7 DV; NAcC, +1.3 AP, +/− 1.4 ML, −5 DV; PFC, +3.2 AP, +/− 0.5 ML, −3.0 DV. A stainless steel obdurator (33GA, Plastics One) was placed inside each cannula.

In order to deliver both drug and laser light to the VTA, we epoxied an optical fiber to a 26GA cannula (McMasters-Carr) at a 10° angle [58]. The cannula terminated 0.5 mm above the tip of the optical fiber so as not to obscure light from the fiber. This cannula+fiber was aimed at the VTA (−5.8 AP, +/−0.7 ML, and −7.7 ventral to brain surface).

IV catheter implantation

Rats were fitted with chronic indwelling jugular catheters (13cm of polyethylene tubing, 0.3mm inner diameter, 0.64 outer diameter; Dow Corning Corporation) for IV drug delivery. One end of the catheter was inserted into the jugular vein and secured in place by silk sutures, the other end passed subcutaneously to a stainless steel guide cannula (Plastics One) that exited the animal's back. Catheters were flushed once daily with 0.1mL of enrofloxacin antibiotic (Baytril, Bayer DVM; 5mg/mL) followed by 0.1mL of heparinized 0.9% physiological saline (50USP/mL).

METHOD DETAILS

Avoidance task

All behavioral procedures were conducted in operant chambers (12.0'' L x 9.5'' W x 8.25''; Med Associates) inside sound-attenuating cabinets. Chambers were fitted with footshock grids, retractable levers, cue lights above the levers, a house light, and speakers for cue tone and white noise. Behavioral programs were controlled by Med PC software.

Rats were initially shaped to press a lever to terminate footshock in single daily 30min sessions. At the start of each session, subjects were presented with a lever, white noise (70dB), and a cue light paired with continuous footshock (0.56mA). A response on the lever resulted in termination of footshock for a 20 s ''safety'' period paired with its own unique discrete cues: the retraction of the lever, dimming of the cue light, illumination of the house light, silencing of white noise, and presentation of a tone (70dB). Subjects were gradually shaped toward the lever by the experimenter until acquisition, upon which an avoidance contingency was introduced.

Subjects received single daily (30min) avoidance training sessions. At trial onset, the response lever was extended and a WS (cue light + white noise) was presented. A response on the lever during the 2 s before the initiation of footshock, was considered an avoidance response and resulted in the retraction of the lever, dimming of the cue light, silencing of white noise, and a 20 s safety period during which the house light was illuminated, a tone persisted and no footshock was delivered. If animals failed to press within this 2 s, recurring footshock was applied (0.5ms, 0.56mA, delivered at 2 s intervals) until the animal responded at which point footshock was terminated and the 20 s safety period was initiated; this was considered an escape response. ''Escape'' and ''avoidance'' responses were tallied and data are presented as the percentage of trials on which rats emitted an avoidance response [(# of avoidance responses per session/ total number of responses in session) *100]. Rats were trained until they reached 50+/−15% (or 80+/−15%) avoidance for two consecutive sessions. Once subjects reached criteria, and at least three weeks after viral transduction, they were tested under the same conditions in conjunction with optogenetic or pharmacological manipulations, and/or voltammetric recording of DA release in the NAcC.

Optogenetic manipulation of avoidance

Before each test session rats were attached to an optical fiber patch cable (MMC28550122C, Fiber Optics for Sale). The cable terminated with bilateral ferrules that were secured to the rat's cranial implant with fitted ceramic split sleeves (SM-CS125S, Precision Fiber Products). The other end of the patch cable attached to a 473nm (for ChR2, 10-15mW; MBL-III-473, Opto Engine) or 532nm (for NPHR, 10-15mW; MGL-III-532, Opto Engine) DPSS laser. Optical stimulation was controlled by Med PC IV (Med Associates) and Tarheel CV software.

Each test session was divided into two segments: a 30min baseline during which animals performed the avoidance task with no laser stimulation, and a 30min laser segment during which each presentation of the WS was accompanied by laser (ChR2: 10 pulses at 20Hz, 5ms pulse width; NPHR: 3 s of stimulation beginning 2 s before WS presentation). The order of baseline and laser stimulation segments were counterbalanced across subjects and days.

Pharmacological manipulation of avoidance

Analysis of performance during our previously implemented 60min optical manipulation avoidance sessions showed that there are no within-session gains in performance ($p > 0.05$; Figure S4). Therefore, we halved the test session length to minimize discomfort and better suit pharmacological manipulations.

IV drug drug delivery was achieved by attaching the animal's catheter cannula to a syringe filled with drug via PE20 tubing. Rimonabant or vehicle (VEH) were delivered IV over 4 s and animals performed on the avoidance task 5min after infusion. For IC infusions, obdurators were removed and replaced by bilateral internal infusion cannula (33GA, Plastics One; VTA: 1mm projection; PFC: 0.5mm projection; NAcc: 1.5mm projection), which were connected to a 5 μL Hamilton syringe via PE50 tubing back-filled with drug. Infusion cannula were inserted 1min prior to drug delivery, drug was delivered in a volume of 0.5 μl/side over 2min using a motorized syringe pump. After each infusion, infusion cannula were left in place for an additional 5min before obdurators were replaced and animals performed in the avoidance task.

In vivo voltammetry

Voltammetric recordings (versus an Ag/AgCl reference electrode) and data acquisition were performed using TarHeel CV software. Animals' electrode implants were attached to custom FSCV equipment via a custom head-stage. Rats received IV VEH and performed the avoidance task for 20min. Next, an IV infusion of 0.56mg/kg rimonabant was delivered and rats performed for an additional 20min, rats then received a final infusion of 0.44mg/kg rimonabant to achieve a cumulative dose of 1.0mg/kg, and performed the task for a final 20min. FSCV procedures and DA signal calibration employed here have been previously described [8, 37].

For FSCV confirmation of optically-evoked DA, rats were transduced with ChR2 and implanted with bilateral optical fibers (as described above). At least three weeks after transduction, animals were anesthetized with isoflurane and implanted with an Ag/AgCl reference electrode and a a glass carbon fiber electrode was lowered into the NAcC (AP:+1.4, ML: −1.4) of the contralateral hemisphere [8]. The glass electrode was driven ventrally until optical stimulation elicited robust DA release (30 pulses; 30Hz). Animals then received trains of optical stimulation consisting of varying pulse number and frequency in a random order (10 pulses at 20, 30, 60 and 90Hz; and 10, 20, and 30 pulses at 30Hz), with at least 5min between each stimulation. Data was collected and compiled with Tarheel CV software and current was translated to DA concentration utilizing a laboratory-generated calibration set.

Drugs for *in vivo* use

The DA D1 receptor antagonist SCH23390 (SCH; 125941-87-9, Sigma-Aldrich) and the DA D2 receptor antagonist Eticlopride (97612-24-3, Sigma-Alrich) were each dissolved in aCSF to one of three doses (0.25 μg/0.5 μl; 0.5 μg/0.5 μl; 1.0 μg/0.5 μl) for IC delivery. Similar doses of SCH diminish responding for positive reinforcers and do not result in locomotor impairments [46, 59–61]. The CB1 antagonist rimonabant (National Institute on Drug Abuse Drug Supply Program) was dissolved in a 1:1:18 mixture of ETOH, alkamuls (EL620, Rhodia Group), and 0.9%physiological saline to either of two doses (0.56mg/0.1mL; 1mg/0.1mL) for IV delivery. Rimonabant was dissolved in a 1:1:18 mixture of ETOH, alkamuls, and aCSF to one of two doses (0.2 μg/0.5 μl; 1.0 μg/0.5 μl) for IC delivery. Similar doses of rimonabant have been utilized by our laboratory to investigate food-maintained responding, and have not been found to affect locomotor behavior [37, 62–65]. The diacylglycerol lipase inhibitor tetrahydrolipstatin (Tocris Bioscience) was dissolved in a 1:1:18 mixture of ETOH, alkamuls, and aCSF to a dose of 5 μg/0.5 μL or 0.5 μg/0.5 μL [31, 66].

Variable time out (VTO) task

TH::Cre+ rats were food restricted to 95% of their free-feeding weight and trained to lever press for food (FR1 with 10 s time out (TO)). Operant chambers were now fitted with a plastic floor with sloped sides, pellet dispenser and pellet receptacle. Food availability following each TO was signaled by illumination of the cue light and the first cued lever press earned the animal one food pellet (14mg chocolate-flavored pellet, Bio-Serv). The session ended when animals reached 25 rewards or after 30min. Rats were trained on this schedule for five sessions after they consistently achieved 25 rewards.

Animals were then transferred to an FR1 with a VTO ranging from 32-60 s (average 46 s). Once animals learned the VTO schedule (i.e., consistently earned 25 rewards), they underwent two test sessions, interleaved with baseline sessions. A digital video recorder above each chamber recoded the animal's behavior. During baseline sessions, animals' optical fiber implants were attached to a 473nm laser via an optical patch cord, but the laser remained off. On Test Session 1, rats received laser stimulation (10 pulses at 20Hz) at the presentation of each cue (cue light illumination). The next day animals performed another baseline session with no laser stimulation. On the final test day (Test Session 2), animals received laser stimulation at the midpoint of each VTO (i.e., not in conjunction with the cue). The connection between the animals' optical implants and the patch cable were insulated to prevent light seepage. Data from each test session was viewed as latency to lever press from either cue-onset or from laser stimulation (Med-PC software). Digital videos of each test session were scored for latency to orient toward the lever (''orient'' was defined as movement of the animal's gaze or body). Video scoring was performed by an experimenter blind to the experimental conditions.

Fear conditioning

Rats underwent a 3-day fear conditioning protocol. On day 1 (conditioning day), animals were placed into an operant box fitted with a footshock grid. Subjects were given 30min to acclimate, after which they were presented with a tone cue three times (20 s tone, 3min ITI), with each presentation culminating in a 2 s scrambled electric footshock of 0.7mA.

Twenty-four hours after conditioning, day 2, rats were placed in a novel cylindrical test chamber (made of plastic and striped radially to provide unique environmental cues) and their optical fiber implants were attached to a 473nm laser via an optical fiber patch cable. Rats were exposed to the tone at 3min intervals for a total of 18 presentations. Throughout each 20 s tone rats received optical stimulation to the VTA (10 pulses at 20Hz, at 2 s intervals).

On day 3, 24 hr later, animals were placed back into the cylindrical test chamber and received 18 tone presentations in the absence of shock and laser. All behavioral sessions were recorded, coded to ensure blind analysis, and hand scored for freezing behavior during each tone. Final data reflect the average scores from two experimenters blind to experimental conditions.

Locomotor testing

A subset of rats from the fear conditioning experiment underwent a single locomotor testing trial. Rats were placed in an operant chamber fitted with a plastic floor with sloped sides. Rats received 20 s of laser stimulation (20Hz, 10 pulses, at 3 s intervals) every 3min for 30min. Test sessions were video recorded and locomotor behavior (distance traveled in cm) was analyzed using EthoVision video tracking software (Noldus).

Ex vivo voltammetry

In vivo FSCV measurements of DA release concurrent with optical stimulation at the electrode tip are beyond the current scope of these technical approaches, so we verified the ability of terminal stimulation to release DA using *ex vivo* voltammetry. Less than one week after avoidance testing, rats were decapitated and brains were quickly removed. 250 μm thick coronal slices containing the NAcC or PFC were placed in carbogen-bubbled, ice-cold modified artificial cerebral spinal fluid (aCSF) containing (in mM): 194 sucrose, 30 NaCl, 4.5 KCl, 1 MgCl2, 26 NaHCO3, 1.2 NaH2PO4, and 10 glucose. All recordings were performed between 290 and 310 mOSm in oxygenated Krebs buffer containing the following (in mM): 126 NaCl, 2.5 KCl, 1.2 NaH2PO4, 2.4 CaCl2, 1.2 MgCl2, 0.4 L-Ascorbic acid, 20 HEPES, 10 Glucose, 25 NaHCO3, and 10 NaOH. A carbon fiber glass electrode was used to record DA release during laser stimulation of NAcC or PFC DA terminals (10 pulses, 20Hz, 473nm laser; 10-15mW).

Slice electrophysiology

TH::Cre+ rats were transduced with ChR2 in the VTA and left undisturbed in their home-cage for 3 weeks or trained on the avoidance task. On test day, rats were decapitated and their brains were rapidly removed and transferred to an oxygenated (95% O_2/ 5% CO_2) ice-cold solution containing: 93mM NMDG, 2.5mM KCl, 1.2mM NaH_2PO_4, 30mM $NaHCO_3$, 20mM HEPES, 25mM Glucose, 5.6mM Ascorbic acid, 3mM Sodium pyruvate, 10mM $MgCl_2$, 0.5mM $CaCl_2$. Horizontal slices containing VTA (220μm) were transferred to a holding chamber filled with oxygenated solution containing: 109mM NaCl, 4.5mM KCl, 1.2mM NaH_2PO_4, 35mM $NaHCO_3$, 20mM HEPES, 11mM Glucose, 0.4mM Ascorbic acid, 1mM $MgCl_2$, 2.5mM $CaCl_2$. Slices were first incubated at 35°C for 10-12 min before transferred to room temperature until the start of the experiments. Slices were transferred to a recording chamber and immersed in oxygenated aCSF containing 126mM NaCl, 3mM KCl, 1.2 mM NaH_2PO_4, 26 mM $NaHCO_3$, 11mM Glucose, 1.5mM $MgCl_2$, 2.4mM $CaCl_2$. The aCSF was flowing (2mL/min) and heated (32-34°C). Slices were visualized with an upright microscope (Olympus, BX51WI) equipped with differential interference contrast (DIC) optics. Recorded neurons were located in the lateral VTA, medial to the terminal nucleus of the accessory optic track and anterior to the third cranial nerve. Whole-cell voltage-clamp recording were acquired using an Axopatch 200B (Molecular Devices) amplifier. Recording pipettes (3-5MΩ) were filled with internal solution containing: 140mM K-gluconate, 2mM NaCl, 1.5 mM $MgCl_2$, 10mM HEPES, 10 mM Tris-phosphocreatine, 4mM Mg-ATP, 0.3mM Na-GTP, 0.1mM EGTA, pH 7.2, 290mOSM. DNQX (20μM), DL-AP5 (40μM), picrotoxin (100 μM), strychnine (1 μM) were present to block AMPA, NMDA, $GABA_A$, and glycine receptors, respectively. $GABA_B$ IPSCs were evoked using optical stimulation (473nm; 3 s; 6-7mW) or electrical stimulation with bipolar tungsten stimulating electrodes with tip separation 300-400μm. A train of six stimuli 100μs duration of 1mA was delivered at 50Hz every 30 s. Stimulation protocols were generated and signals acquired using the WinLTP program. Control $GABA_B$ IPSCs were recorded for 10min before the CB1 receptor blocker AM251 (2μM) was applied for an additional 30min. Data are presented as the change in percent from control traces.

LC-MS/MS

Rats were anesthetized with isoflurane gas and placed in a stereotaxic frame for intracranial infusion of THL (n = 9) or VEH (n = 9) into the VTA. Five minutes after infusion, animals were decapitated, their brains were removed, quickly chilled and a 1mm punch of VTA tissue was taken. Tissue was frozen with dry ice and stored at −80°C until analysis. Liquid chromatography-tandem mass spectrometry was used to quantify 2-AG in brain tissue. Samples were homogenized in methanol containing a deuterated standard (Cayman Chemicals) and 0.1% formic acid, bath sonicated at 4C for 10 min, incubated at −20°C overnight, and centrifuged. Water was added to the supernatant for a final ratio of 75:25 Methanol:Water. Samples (20 μl) were injected onto a C-18 column (50 × 2 mm, 1.7 μm; Acquity) at 35C under the following gradient: 40% A (water) and 60% B (2:1 Acetonitrile:Methanol) from 0 to 0.25min, increased to 5% A and 95% B from 0.25 to 3.75min held for 2min, and returned to 40% A and 60% B from 5.75 to 6min. Both mobile phase components contained 0.1% formic acid (v/v). A QTrap 6500 mass spectrometer (Sciex) was used to detect analyte via selective reaction monitoring in the positive ion mode using the following reactions (the mass in parentheses represents the mass of the deuterated internal standard): (m/z 379(384) → 287(287)). Quantification was achieved via stable-isotope dilution.

Histology

Rats were deeply anesthetized with isoflurane and trans-cardially perfused with phosphate-buffered saline (PBS; 0.1M) and paraformaldehyde (4%). Brains were removed and stored in PBS at 4°C. Brains were sliced coronally (40 μm) and mounted on slides for EYFP visualization (Figure S5). Animals that did not show viral expression in the target region or misplacement of cannula were removed from data analysis.

For tyrosine hydroxylase (TH) immunohistochemistry, 40μm brain sections were collected in individual wells filled with phosphate buffered saline (PBS; 1M). Sections were washed with PBS between each step. Sections were incubated for 30min with 3% normal donkey serum (Jackson Labs) in 0.2% Triton X with PBS to block nonspecific binding, and then incubated for 24 hr with TH primary antibody (TH-mouse; 1:500; Frontier Institute) and the GFP primary antibody (GFP-Chicken; 1:4000; Aves Labs) in 3% donkey serum in 0.2% Triton X with PBS. Sections were then incubated for 12 hr in the secondary antibodies donkey anti-chicken (1:1000; Jackson Labs) and donkey anti-mouse (1:1000; Jackson Labs). Finally, sections were incubated with 4',6-diamidino-2-phenylindole (DAPI; 0.1 μl/mL PBS; Sigma) for 30min to mark nucleic acid. Sections were then mounted onto slides, dehydrated and coverslipped. Implant placement and viral and immunohistochemical expression (fluorescence) was imaged on an Olympus BX61 confocal microscope (Figure S6). Inspection confirmed expression of ChR2 virus in TH+ processes. This has also been confirmed by other groups [11, 67, 68].

QUANTIFICATION AND STATISTICAL ANALYSIS

Appropriate parametric statistics were utilized to test our hypotheses. If the data did not meet the assumptions of the intended parametric test (normality, heterogeneity of variance tests) appropriate non-parametric tests were used to confirm the results. Power analysis assumptions were: power = 0.9; alpha = 0.5; two-tailed and an expected difference 50% greater than the observed standard deviation.

We utilized SPSS (IBM) and Prism (GraphPad Software, CA) for analysis and graph generation. Effects of optogenetic manipulations during avoidance were examined using two-way genotype x stimulation ANOVAs with repeated-measures on stimulation (i.e., Baseline or Laser). Comparisons of avoidance following drug administration were assessed with one-way repeated-measures ANOVAs on treatment (i.e., dose and presence of laser stimulation). Fisher's Least Significant Difference post hoc tests were used to examine main effects and interactions when more than two treatments were examined. When fewer than three treatments were administered to each animal, paired-samples t tests with Bonferroni correction were employed to assess within subjects effects and independent samples t tests with Bonferroni correction were employed to examine between subjects effects. All t tests were two-tailed unless a hypothesis was clearly directional based upon other published work. VTO data was analyzed using a one-way repeated-measures ANOVA on trial type (e.g., baseline versus laser at cue or laser during the VTO). Freezing and locomotor behavior was analyzed with two-way (trial x genotype) repeated-measures ANOVAs. FSCV data was analyzed by ANOVA with repeated-measures. The effects of VEH versus THL administration on tissue eCB levels were analyzed with independent samples t tests. Measurements of IPSCs were made using pClamp software (Molecular Devices). IPSC data are reported as percent of baseline. Between groups repeated-measures ANOVA was used to assess IPSCs following avoidance training.